Anal. Chem. **2011,** *83,* 231–239

Enrichment of $H_2{}^{17}O$ from Tap Water, Characterization of the Enriched Water, and Properties of Several ^{17}O-Labeled Compounds

Brinda Prasad, Andrew R. Lewis, and Erika Plettner*

Department of Chemistry, Simon Fraser University, 8888 University Drive, Burnaby, BC, Canada - V5A 1S6

Dioxygen, O_2, is central in many processes of life, such as photosynthesis and respiration. Many of the enzymatic mechanisms in anabolic and catabolic processes require O_2 and generate oxygen-containing intermediates or products. Examples of enzymes that require oxygen atoms at some point in their catalytic cycles, either as O_2, superoxide, H_2O_2, or water, include three important groups. First are the heme-containing enzymes, such as cytochromes P450,[1,2] cyclooxygenase,[3,4] dioxygenases,[5,6] or NO synthases.[7] Second are flavin-containing oxidoreductases,[8] such as putrescine oxidase or Baeyer−Villigerases,[9] and third are nonheme iron-containing enzymes, such as fatty acid desaturases.[10] Despite its high (1.229 V) oxidation potential, dioxygen is not very reactive under standard conditions in living organisms because O_2 is in the triplet ground state, whereas most metabolites are in a singlet ground state. The superoxide ion, $O_2^{-\cdot}$, is formed through a one-electron reduction of O_2. Upon a further reduction and protonation, superoxide forms hydrogen peroxide, H_2O_2, a mild oxidant or reductant.[11] Further reduction and protonation yields water, the least reactive oxygen species in this chain. The enzymes listed above exploit the differential reactivities in this chain of oxygen species, from O_2 to water in their catalysis. The reduction of O_2 to water ($O_2 + 4e^- + 4H^+ \rightarrow 2\ H_2O$, $\Delta G = -474$ kJ/mol)[12] is highly exothermic, and cytochromes P450 or fatty acid desaturases exploit this property, utilizing the free energy released in the reduction of O_2 to activate hydrocarbon C−H bonds. These enzymes accomplish this feat of thermodynamic coupling by coordinating with O_2 and reducing it in a stepwise manner. Some reactive oxygen species are sometimes released prematurely from these enzymes, leading to oxidative stress in the cell.[13] It is, therefore, of interest to study how the various oxygen species interact with enzymes.

Oxygen has three stable isotopes: ^{16}O (abundance 99.759%), ^{17}O (0.037%) and ^{18}O (0.204%). ^{16}O and ^{18}O have a nuclear spin (I) of zero whereas ^{17}O has $I = 5/2$ which makes it detectable by NMR spectroscopy.[14] Pure $H_2{}^{17}O$ is the commonly accepted reference standard[15] for the chemical shifts in ^{17}O NMR. ^{17}O

* To whom correspondence should be addressed. Tel: (+1)-778-782-3586. Fax: (+1)-778-782-3765. E-mail: plettner@sfu.ca.

(1) Schlichting, I.; Berendzen, J.; Chu, K.; Stock, A. M.; Maves, S. A.; Benson, D. E.; Sweet, R. M.; Ringe, D.; Petsko, G. A.; Sligar, S. G. *Science* **2000**, *287*, 1615–1622.
(2) Yamamoto, H.; Yatou, A.; Inoue, K. *Phytochemistry* **2001**, *58*, 671–676.
(3) Amma, H.; Naruse, K.; Ishiguro, N.; Sokabe, M. *Br. J. Pharmacol.* **2005**, *145*, 364–373.
(4) Kuehn, H. S.; Swindle, E. J.; Kim, M. S.; Beaven, M. A.; Metcalfe, D. D.; Gilfillan, A. M. *J. Immunol.* **2008**, *181*, 7706–7712.
(5) Wang, P.; Zhang, W. J.; Zhan, J. X.; Tang, Y. *Chembiochem* **2009**, *10*, 1544–1550.
(6) Werner, E. R.; Werner-Felmayer, G. *Curr. Drug Metab.* **2007**, *8*, 201–203.
(7) Lamkin-Kennard, K. A.; Buerk, D. G.; Jaron, D. *Microvasc. Res.* **2004**, *68*, 38–50.
(8) Valton, J.; Mathevon, C.; Fontecave, M.; Niviere, V.; Ballou, D. P. *J. Biol. Chem.* **2008**, *283*, 10287–10296.
(9) Tanner, A.; Hopper, D. J. *J. Bacteriol.* **2000**, *182*, 6565–6569.
(10) Nakagawa, Y.; Ueda, A.; Kaneko, Y.; Harashima, S. *Mol. Genet. Genom.* **2003**, *269*, 370–380.
(11) Sawyer, D. T.; Roberts, J. L. *J. Electroanal. Chem.* **1966**, *12*, 90–&.
(12) Castellan, G. W. *Phys. Chem.* **1983**, 381.
(13) Kadkhodayan, S.; Coulter, E. D.; Maryniak, D. M.; Bryson, T. A.; Dawson, J. H. *J. Biol. Chem.* **1995**, *270*, 28042–28048.
(14) Zhu, J.; Kwan, I. C.; Wu, G. *J. Am. Chem. Soc.* **2009**, *131*, 14206–14207.
(15) Greenzai, P.; Luz, Z.; Samuel, D. *J. Am. Chem. Soc.* **1967**, *89*, 749–&.

10.1021/ac1022887
Published on Web 12/03/2010

chemical shifts span a range −30 to +600 ppm[16] which makes distinguishing functional groups containing oxygen (bonded to carbon, nitrogen, or sulfur) relatively straightforward, despite the low abundance and high cost of ^{17}O. Due to the lack of interferences, enzymatic samples can, in principle, be studied directly by ^{17}O NMR without the need to remove the protein, making it a practical tool for mechanistic studies. ^{17}O NMR studies have enormous applications in chemistry and biology. For example, Gullion et al.[17] have reported the determination of secondary structures in polyamides by $^{13}C-^{17}O$ READPOR NMR. ^{17}O NMR is also used in imaging analysis to determine the cerebral metabolic rate of oxygen in rats.[18]

Commercially available $H_2{}^{17}O$ is prohibitively expensive (1 g of 90% enriched $H_2{}^{17}O$ costs >$2000), and in order to facilitate and expand the use of ^{17}O-labeling studies in enzymatic reactions, there is a need for an economical method by which researchers can enrich ^{17}O from water and characterize the isotopic enrichment in a simple and reliable way. In this paper we describe an inexpensive method for enriching both $H_2{}^{17}O$ and $H_2{}^{18}O$ in tap water using slow evaporation followed by fractional distillation. We also report simple procedures to determine the percentage of isotopic enrichment of ^{17}O-labeled water using gas chromatography−mass spectroscopy (GC-MS) of 1-hexanol and hexamethyldisiloxane (HMDS) synthesized from $H_2{}^{17}O$ and deionized water. The fractional distillation method reported here is based on the differences in the volatility of the three forms of water that vary in their oxygen isotope.[19−21]

In our research group we use the isotope-enriched water for the study of enzymatic reactions of $P450_{cam}$, a camphor hydroxylase. We therefore also describe the preparation of ^{17}O-labeled hydrogen peroxide by the electrolysis of $H_2{}^{17}O$, synthesis of ^{17}O-labeled camphor and report the ^1H, ^{13}C, and ^{17}O NMR data for ^{17}O 1-hexanol, ^{17}O camphor, ^{17}O trimethylsilanol, and ^{17}O hexamethyldisiloxane. Furthermore, while studying the labeled camphor in $H_2{}^{17}O$, we detected an unusual ^{17}O exchange into the ethanol that was used to deliver camphor into the water. This is an important example that illustrates how ^{17}O NMR can provide insight into reactions that may otherwise have gone unnoticed.

EXPERIMENTAL SECTION

Enrichment of $H_2{}^{17}O$ from Tap Water. Tap water (~1−2 L) was placed in a shallow black bowl and left to evaporate slowly at room temperature on a windowsill. When the water in the bowl reached ca. 20−50 mL, it was collected into a measuring cup and briefly boiled in a microwave (~30 s high power) to kill any bacteria that may have accumulated. The sterilized enriched water was stored in a glass jar with a tight lid. This process was repeated until more than 1 L of enriched water had been accumulated. The water was filtered through fluted filter paper (Whatman Cat. No.1001-070), to remove any particulate matter, and ~500 mL of this was placed in a 1 L round-bottom flask, fitted with two condensers (Supporting Information Figure S1), for fractional distillation.

Fractional Distillation of the Enriched Water. The vertical condenser was packed with glass wool and was not cooled with running water. The tilted condenser at the top had cold water running to condense the distillate. The system was attached to a single-neck still head that could be rotated easily in order to allow various fractions of water to be collected without interrupting the distillation. The distillation source flask was heated with a mantle connected to a Variac (setting: 50). To ensure good fractionation, it was important that the water was not heated too quickly.

The boiling point was monitored using a thermometer at the top of the fractionation column (Supporting Information Figure S1), and several fractions with different boiling points were collected. Temperatures given are not corrected. For reference, the SFU Burnaby campus lies 370 m above sea level, and the boiling point of tap water registers at 97 °C in our apparatus at this location. Fractions having boiling points of 98.5 °C (10 mL × 6) and 99 °C (10 mL) were collected.

Preparation of Hydrogen Peroxide by the Electrolysis of Water. Hydrogen peroxide is a redox-active compound that is most commonly encountered as an oxidant.[22] Industrially, anthaquinone is hydrogenated to form anthrahydroquinone which is further oxygenated to form hydrogen peroxide.[23] Other methods for synthesizing H_2O_2 include hydrolysis of peracids (e.g., peracetic acid),[24] and enzymatic hydrolysis of phosphatidic acid to glycerol-3-phosphate (G3P), which is then oxidized by G3P oxidase to hydrogen peroxide.[25] Catalytic methods of production using palladium membranes[26] and zirconium catalysts[27] have also been reported. Several electrolytic methods for hydrogen peroxide generation have been reported in the literature, including a fuel-cell method,[28−30] electrolysis of water using a carbon cathode, and a RuO_2-based titanium anode,[31] using a solid-polymer electrolyte[32] or using a proton-exchange membrane.[33] We required a method that uses H_2O, and so we selected electrolysis.

In our method, the electrolysis of 5 mL of $H_2{}^{17}O$ buffered to pH 7.7 using 50 mM phosphate buffer (made from 50 mM KH_2PO_4 and 50 mM K_2HPO_4) with 150 mM KCl was carried out using a copper cathode and a graphite anode. The electrodes were connected to a Biorad Power Pac 1000 and a

(16) Boykin, D. W. *^{17}O NMR spectroscopy in organic chemistry*; CRC Press: Boca Raton, FL, 1991.
(17) Gullion, T.; Yamauchi, K.; Okonogi, M.; Asakura, T. *Macromolecules* **2007**, *40*, 1363–1365.
(18) Zhu, X. H.; Zhang, Y.; Tian, R. X.; Lei, H.; Zhang, N. Y.; Zhang, X. L.; Merkle, H.; Ugurbil, K.; Chen, W. *Proc. Natl. Acad. Sci. U.S.A.* **2002**, *99*, 13194–13199.
(19) Sakata, S.; Morita, N. *Bull. Chem. Soc. Jpn.* **1957**, *30*, 254–259.
(20) Randall, M.; Webb, W. A. *Ind. Eng. Chem.* **1939**, *31*, 227–230.
(21) Sakata, S.; Morita, N. *Bull. Chem. Soc. Jpn.* **1956**, *29*, 284–285.
(22) Anh, D. T. V.; Olthuis, W.; Bergveld, P. *Sens. Actuators, B* **2003**, *91*, 1–4.
(23) Kirchner, J. R. *Kirk-Othmer Encyclopedia of Chemical Technology*; Grayson, M., Eckroth, D., Eds.; Wiley: New York, 1979; Vol. 13, pp 12−38.
(24) Greenspan, F. P.; Mackellar, D. G. *Anal. Chem.* **1948**, *20*, 1061–1063.
(25) Morita, S.; Ueda, K.; Kitagawa, S. *J. Lipid Res.* **2009**, *50*, 1945–1952.
(26) Choudhary, V. R.; Gaikwad, A. G.; Sansare, S. D. *Angew. Chem., Int. Ed.* **2001**, *40*, 1776–1779.
(27) Melada, S.; Rioda, R.; Menegazzo, F.; Pinna, F.; Strukul, G. *J. Catal.* **2006**, *239*, 422–430.
(28) Otsuka, K.; Yamanaka, I. *Electrochim. Acta* **1990**, *35*, 319–322.
(29) Xu, F. Y.; Song, T. S.; Xu, Y.; Chen, Y. W.; Zhu, S. M.; Shen, S. B. *J. Rare Earths* **2009**, *27*, 128–133.
(30) Yamanaka, I.; Onizawa, T.; Takenaka, S.; Otsuka, K. *Angew. Chem., Int. Ed.* **2003**, *42*, 3653–3655.
(31) Drogui, P.; Elmaleh, S.; Rumeau, M.; Bernard, C.; Rambaud, A. *J. Appl. Electrochem.* **2001**, *31*, 877–882.
(32) Yamanaka, I.; Murayama, T. *Angew. Chem., Int. Ed.* **2008**, *47*, 1900–1902.
(33) Tatapudi, P.; Fenton, J. M. *J. Electrochem. Soc.* **1993**, *140*, L55–L57.

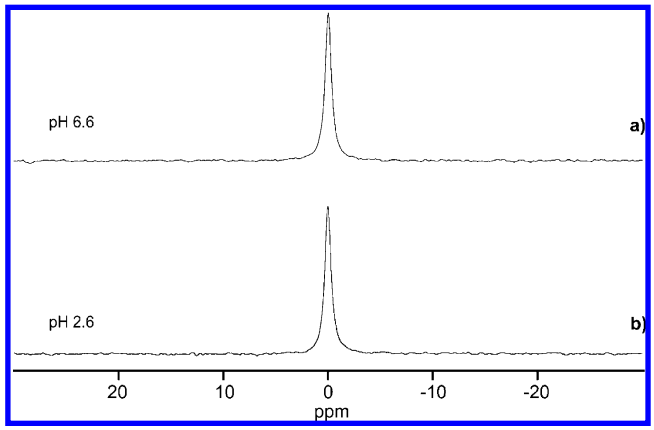

Figure 1. ^{17}O NMR spectrum of water samples: (a) pH 6.6, (b) pH 2.6.

Scheme 1. Formation of ^{17}O-Labeled Hexanol by a S_N2 Reaction

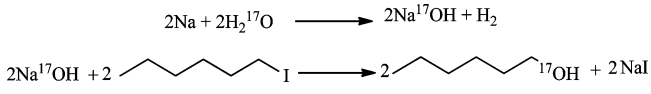

constant voltage of 5 V was applied for one hour. The reaction was monitored by observing the redox properties of H_2O_2 in two different reactions (quantitation details of H_2O_2 in the Supporting Information).

^{17}O NMR of Water. The proton decoupled ^{17}O NMR of the water sample (pH 6.6) was obtained with $CDCl_3$ lock in a coaxial capillary, recycle delay 0.2 s and the chemical shift was set to 0 ppm. (Figure 1a). Another $H_2{}^{17}O$ sample containing buffer (pH 2.6) was also run in the same fashion to see if there is any variation in the chemical shift with pH. (Figure 1b). NMR acquisition conditions are included in the experimental details of the Supporting Information.

Synthesis of Labeled 1-Hexanol and Hexamethyldisiloxane. The ^{17}O-labeled water could not be run directly on a gas chromatograph−mass spectrometer because the fused-silica capillary column would have been damaged by the water. We chose to prepare labeled 1-hexanol because smaller alcohols are hard to detect by GC-MS (weak molecular ion peak and high volatility) and higher alcohols give more complex fragmentation patterns. ^{17}O-Labeled hexanol was synthesized by reacting the ^{17}O-enriched water with sodium metal, followed by addition of 1-iodohexane. Briefly, 200 μL (0.2 mmol) of ^{17}O water was reacted with 3 mg (0.13 mmol) of sodium metal (Scheme 1). When the metal had all reacted, 1 equiv of 1-iodohexane (10 μL was dissolved in 100 μL of acetone) was added, and the reaction mixture was stirred at room temperature for 3 h. The reaction was monitored every 30 min by GC-MS, and after 3 h, complete depletion of 1-iodohexane was observed.

A solution (1 μL diluted 1000-fold with distilled hexane) of the 1-hexanol was injected into a Varian 3800 GC, equipped with a 30 m SPB-5 column (i.d. = 0.25 mm, 0.25 μm film thickness, Supelco) interfaced with a Varian Saturn 2000 ion trap mass spectrometer. The trimethylsilyl ether of 1-hexanol was prepared by reacting 0.5 μL of 1-hexanol in a small ampule with 4 μL of bis(trimethylsilyl)triflouroacetamide (BSTFA, Sigma) for 40 min

Scheme 2. Hydrolysis Reaction of BSTFA To Form Hexamethyldisiloxane (HMDS)

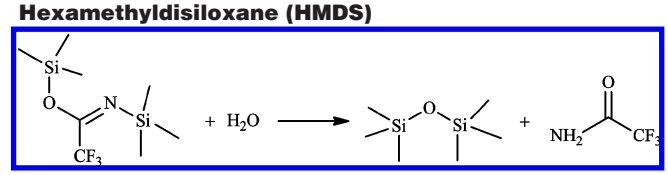

at RT, and the reaction mixture was diluted with hexane (1000×) for the injection of 1 μL on the GC-MS. (The column oven settings are included in the experimental details of the Supporting Information).

To form hexamethyldisiloxane, HMDS (or bis-trimethylsilyl oxide) (Scheme 2), 0.5 μL of deionized water and $H_2{}^{17}O$ were each treated with 5 μL of BSTFA for 40 min at 60 °C. For HMDS GC-MS analysis, ion storage (SIS mode) was used, and m/z 135−150 amu was scanned. For ^{17}O NMR studies, 300 μL of BSTFA was treated with 25 μL of $H_2{}^{17}O$ in a small ampule and left overnight at RT. About 300 μL of pentanol was added the next day, the organic extract was concentrated at RT, and 450 μL of $CDCl_3$ was added. In our NMR studies, ^{17}O-labeled trimethylsilanol, ^{17}O-labeled hexamethyldisiloxane (HMDS), and ^{17}O-labeled trifluoroacetamide (reaction byproduct) were detected.

Preparation of ^{17}O Camphor. Camphor (7 mg) was dissolved in 0.5 mL of $CDCl_3$ and added to 50 μL of $H_2{}^{17}O$ buffer (50 mM phosphate, pH 7.7) in an NMR tube (diameter: 5 mm). The mixture was left to react at room temperature overnight and analyzed directly by ^{17}O NMR the next day. After NMR, a sample was extracted and checked by EI GC-MS (The GC-MS data of ^{17}O-labeled camphor is included in the Supporting Information).

RESULTS AND DISCUSSION

Density and Refractive Index. The density and refractive index experimental details are included in the Supporting Information. The density of deionized water was found to be 0.9986 ± 0.0006 g/cm^3 and of $H_2{}^{17}O$ fraction 11 (99%) 1.0026 ± 0.0010 at 21 °C. This increase in density for $H_2{}^{17}O$ is significant (P = 0.014, t test, five replicates) and expected from the observation that $H_2{}^{18}O$ (99 atom ^{18}O%) has a reported density of 1.11 g/mL at 20 °C.[34]

The refractometer was calibrated with ethanol whose refractive index was found to be 1.3605, as reported in the literature.[35] For deionized water, the refractive index was measured to be 1.3321, and for $H_2{}^{17}O$, it was 1.3318. The literature value for $H_2{}^{16}O$ is reported to be 1.3330.[36] The refractive index of $H_2{}^{17}O$ has not been reported previously according to our knowledge.

Determination of the Percentage of $H_2{}^{17}O$ in the Fractions from Distillation. We prepared two compounds to assess the percentage of $H_2{}^{17}O$ in the fractions obtained from distillation: 1-hexanol and hexamethyldisiloxane (HMDS). The percentage of labeling was calculated using the integrated peak areas of the molecular ion ($M^{+\cdot}$, for 1-hexanol) or a prominent fragment ion (M − 16, for HMDS) of

(34) Sigma-Aldrich catalogue, 2009−2010, p 2713.
(35) Raty, J.; Keranen, E.; Peiponen, K. E. *Meas. Sci. Technol.* **1998**, *9*, 95–99.
(36) Kim, Y. C.; Banerji, S.; Masson, J. F.; Peng, W.; Booksh, K. S. *Analyst* **2005**, *130*, 838–843.

Scheme 3. Fragmentation Analysis of Hexamethyldisiloxane under GC-MS Conditions

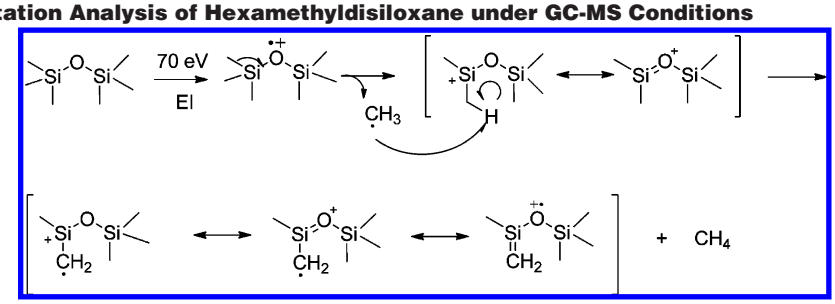

nonlabeled and ^{17}O-labeled compounds. The natural isotope abundance corrections were done by using nonlabeled compound standards.

For nonlabeled 1-hexanol, the natural abundance of the M + 1 mass can be calculated by:

$$L_{nat} = \frac{A_{175}}{A_{174} + A_{175}} \times 100$$

where L_{nat} is the natural abundance of the M + 1 peak in the mass spectrum (due to ^{13}C, ^{2}H, and ^{17}O), A_{175} is the area of the peak with m/z 175 (M + 1) at the retention time of 1-hexanol, and A_{174} is the area of the peak with m/z 174 ($M^{+\cdot}$).

The percentage of ^{17}O in labeled hexanol is:

$$L_{17gross} = \frac{A_{175}}{A_{174} + A_{175}} \times 100$$

The net percentage of ^{17}O in the tested 1-hexanol is:

$$L_{17net} = (L_{17gross} - L_{nat})$$

The labeling of ^{17}O in 1-hexanol was found to be 94.07% by this method. To obtain another ^{17}O-labeled compound from water, we treated water (deionized $H_2{}^{16}O$, $H_2{}^{17}O$) and the residue from the fractional distillation (which should contain large quantities of $H_2{}^{18}O$) with BSTFA to obtain the BSTFA hydrolysis product hexamethyldisiloxane (HMDS). The percentages of ^{17}O and ^{18}O in HMDS can be calculated in the same fashion as described for 1-hexanol, except that the relevant ion is M − CH_4 (Scheme 3), i.e., 146 (for ^{16}O), 147 (for ^{17}O), and 148 (for ^{18}O).

The natural abundances of one or two extra mass units are L_{nat+1} and L_{nat+2} are, respectively.

$$L_{nat+1} = \frac{A_{147}}{A_{146} + A_{147} + A_{148}} \times 100 L_{nat+2} = \frac{A_{148}}{A_{146} + A_{147} + A_{148}} \times 100$$

The gross labeling in HMDS from the distillate can be calculated by:

$$L_{gross+1} = \frac{A_{147}}{A_{146} + A_{147} + A_{148}} \times 100 L_{gross+2} = \frac{A_{148}}{A_{146} + A_{147} + A_{148}} \times 100$$

Table 1. Percentage of Oxygen Isotopes (^{16}O, ^{17}O and ^{18}O) and Boiling Points for the Water Samples Obtained from the Fractional Distillation

sample	boiling point (°C)[a]	approx. vol (mL)	% ^{16}O[b]	% ^{17}O[c]	% ^{18}O[d]
deionized water	97.0	–	99.7	0.1	0.2
fraction #5	98.5	60	0.2	99.1	0.7
fraction #11	99.0	10	ND[e]	99.7	0.3
residue	–	~100	13.0	29.7	57.3

[a] The boiling points of the water fractions collected from the fractional distillation. [b] Percentage of the ^{16}O isotope. [c] Percentage of the ^{17}O isotope. [d] Percentage of the ^{18}O isotope. [e] ND = Not detected.

The net ^{17}O in HMDS is:

$$L_{17net} = (L_{gross+1} - L_{nat+1})$$

and the net ^{18}O in HMDS is:

$$L_{18net} = (L_{gross+2} - L_{nat+2})$$

In the trimethylsilyl (TMS)-containing compounds, ^{29}Si (natural abundance relative to ^{28}Si, 5.10%) makes a contribution to the "+1" mass peak and ^{30}Si (abundance 3.35%) makes a significant contribution to the "+2" mass peak.[37] The results of this analysis are shown in Table 1. The higher the boiling point of a fraction, the higher the ^{17}O content in the distillate. As expected, the residue contained a high percentage of $H_2{}^{18}O$.

^{17}O NMR. *Water.* The effect of dissolved ions on the ^{17}O chemical shift of water has been described by Li et al.[38,39] who measured the ^{17}O chemical shift of $H_2{}^{17}O$ with HCl and NaOH concentrations ranging from 0 to 1.0 mol/L. They reported a linear correlation between the ^{17}O chemical shift and the acid (or base) concentration. These authors also demonstrated the effect of concentration of NaCl, KCl, Na_2CO_3, $NaHCO_3$, Na_2SO_4, and $MgSO_4$ on the ^{17}O chemical shift of $H_2{}^{17}O$ and observed a linear variation in all cases.

We measured the ^{17}O chemical shift of water for a series of samples adjusted to various pH values using dilute phosphate buffers (buffer concentration was kept constant) and did not observe any variation (Figure 1a and 1b).

Sodium Hydroxide, Hexanol, HMDS, Trimethylsilanol, and Trifluoroacetamide. The ^{17}O chemical shift of labeled sodium

(37) Silverstein, R. M.; Bassler, G. C.; Morrill, T. C. *Spectrometric Identification of Organic Compounds*; John Wiley & Sons: New York, 1981; p 10.
(38) Li, R. H.; Jiang, Z. P.; Shi, S. Q.; Yang, H. W. *J. Mol. Struct.* **2003**, *645*, 69–75.
(39) Li, R. H.; Jiang, Z. P.; Yang, H. W.; Guan, Y. T. *J. Mol. Liq.* **2006**, *126*, 14–18.

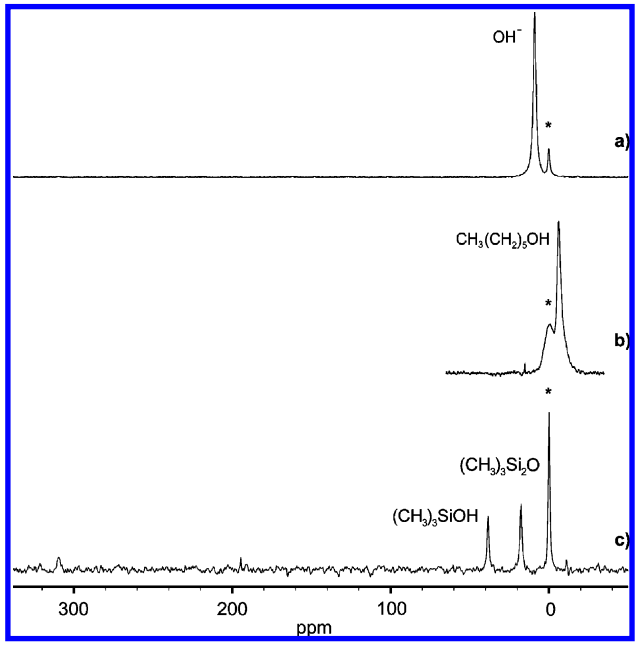

Figure 2. ^{17}O NMR spectra of (a) labeled sodium hydroxide, (b) labeled 1-hexanol, (c) labeled trimethylsilanol, and hexamethyldisiloxane. The $H_2{}^{17}O$ peak (marked *, set to 0 ppm) is an external standard and was used to calibrate the chemical shift scales.

Scheme 4. Exchange of Labeled Trifluoroacetamide as a Side Product in BSTFA Hydrolysis of Water

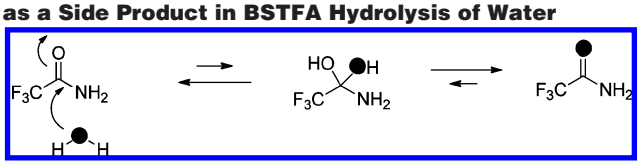

hydroxide (~0.5 M) was 8.8 ppm (Figure 2a). The chemical shifts of other ^{17}O-labeled compounds were −4.16 ppm for 1-^{17}O-hexanol (Figure 2b), 38.5 ppm for ^{17}O-HMDS (Figure 2c), 17.7 ppm for trimethylsilanol (Figure 2c), and 310.0 ppm for trifluoroacetamide (Figure 2c). Formation of the latter compound during the hydrolysis of BSTFA suggests that the amide carbonyl oxygen can exchange with the oxygen from added water (Scheme 4). The chemical shifts of trimethylsilanol in acetone-d_6 was reported to be 12.6 ppm which agrees with our result.[40]

Camphor. To further explore the NMR properties of the ^{17}O label, camphor was exchanged with ^{17}O-enriched water. The ^{17}O chemical shift of this camphor solution dissolved in $CDCl_3$ was 502.4 ppm (Figure 3a) (Scheme 5). When a 1 M ^{17}O-labeled camphor solution in ethanol was exchanged with ^{17}O-enriched water, the chemical shift of camphor was found to be 499 ppm (Figure 3b) (Scheme 6a). The camphor peak seemed to be small, and surprisingly an intense peak at 11 ppm (Figure 3b) was also observed which corresponds to ^{17}O-labeled ethanol. Previous literature studies for primary and secondary alcohols suggest a chemical shift of −3 to +10 ppm.[41] The chemical shift was confirmed with a control experiment in which ethanol was dissolved in $H_2{}^{17}O$, and a similar peak at 11 ppm was observed due to slow exchange. (Figure 3c) (Scheme 6b). Surprisingly, the intensity of this peak was significantly smaller than in the

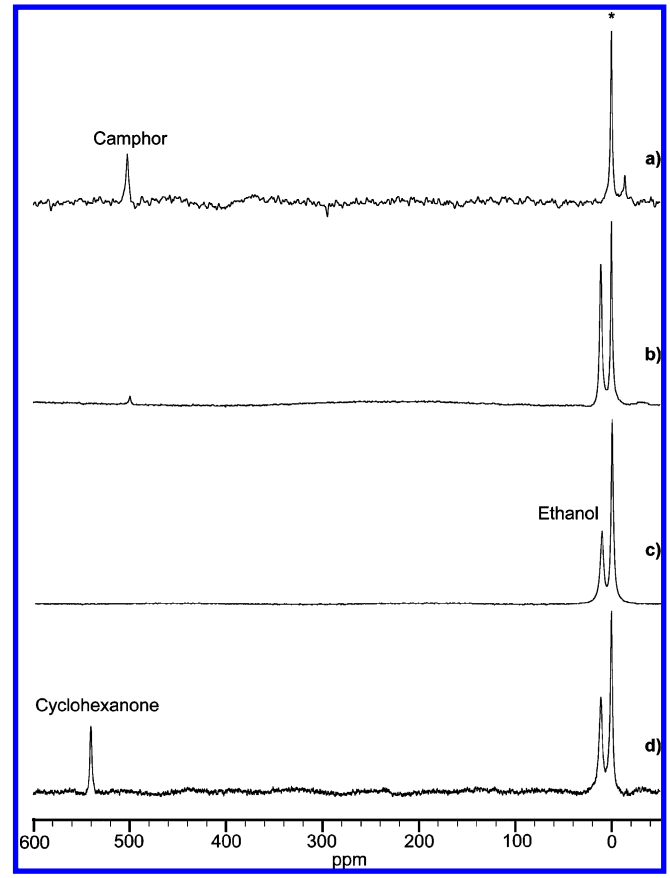

Figure 3. ^{17}O NMR spectra of (a) labeled camphor dissolved in $CDCl_3$ with an external $H_2{}^{17}O$ standard (*), (b) labeled camphor dissolved in ethanol with $H_2{}^{17}O$, (c) labeled ethanol with $H_2{}^{17}O$, and (d) labeled cyclohexanone dissolved in ethanol with $H_2{}^{17}O$ added.

Scheme 5. Formation of Labeled Camphor in $CDCl_3$

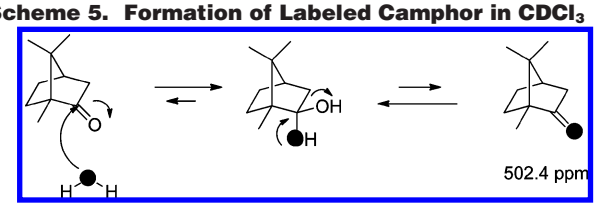

presence of camphor. This suggests that labeled ethanol formation can occur due to its exchange with $H_2{}^{17}O$ and also when ethanol attacks the keto group of ^{17}O-labeled camphor, to form the hemiacetal of camphor. An attack of $H_2{}^{17}O$ on C-1 of ethanol can then take place, and when the hemiacetal collapses, labeled ethanol is formed. To determine if a similar nucleophilic attack on hemiacetal moieties can happen for ketones less strained than camphor, a 1 M solution of cyclohexanone in ethanol was exchanged with $H_2{}^{17}O$ (Figure 3d) (Scheme 6c), and two peaks appeared: one at 540 ppm corresponding to the labeled cyclohexanone as reported in the literature[16] and another at 11 ppm corresponding to labeled ethanol. The intensity of the ketone peak for labeled cyclohexanone was higher than that of labeled camphor. Conversely, the intensity of labeled ethanol was smaller relative to water in the cyclohexanone sample than in the camphor reaction mixture, suggesting that camphor catalyzes the exchange of the ethanol OH group more effectively than cyclohexanone. A possible reason for this could be that the camphor carbonyl carbon is more electrophilic than that of cyclohexanone, because of strain

(40) Cerkovnik, J.; Tuttle, T.; Kraka, E.; Lendero, N.; Plesnicar, B.; Cremer, D. *J. Am. Chem. Soc.* **2006**, *128*, 4090–4100.
(41) Alam, T. M.; Click, C. A. *Spectrosc. Lett.* **1998**, *31*, 587–594.

Scheme 6. (a) Reaction of Camphor Solution in Ethanol with ^{17}O-Enriched Water. (b) Reaction of Ethanol with ^{17}O -Enriched Water. (c) Reaction of Cyclohexanone Solution in Ethanol with ^{17}O-Enriched Water

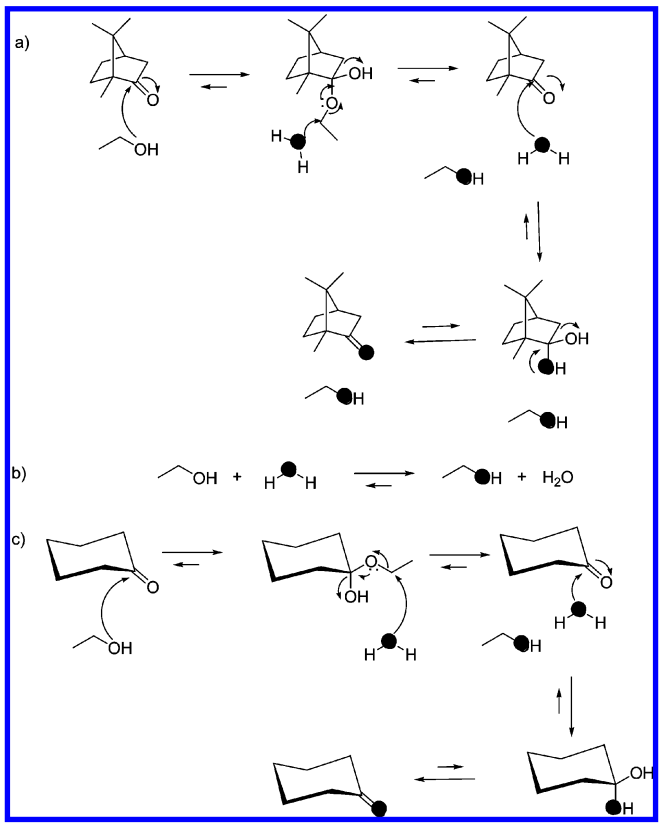

in the bicyclic ring system.[42] This would cause the hemiacetal to form more readily with camphor than with cyclohexanone, and a higher concentration of hemiacetal would lead to a higher probability of alcohol exchange reaction. Thus, the carbonyl exchange reaction is potentially useful for the labeling of compounds, but it also needs to be taken into account when studying metabolic pathways by oxygen labeling.

Hydrogen Peroxide. For our research with P450, we also prepared labeled $H_2{}^{17}O_2$ by electrolysis. The hydrogen peroxide had an ^{17}O chemical shift of 179 ppm (Figure 4), in agreement with the value previously reported in the literature.[43]

Formation of Labeled Alcohols by Exchange with $H_2{}^{17}O$ Involves a S_N2 Mechanism. To determine whether the ethanol OH exchange reaction shown in Scheme 6 does involve attack of water on the primary alcohol carbon, the exchange reaction of camphor dissolved in hexanol with $H_2{}^{17}O$ was tried. If attack of water occurs with concomitant expulsion of the camphor oxygen (Scheme 7), then 1-hexanol should form cleanly. If, however, the reaction involves the formation of a carbocation (i.e., if attack 'b' in scheme 7 occurs prior to attack 'a'), then 2-hexanol should form by rearrangement of the primary carbocation. The reaction yielded labeled hexanol by ^{17}O NMR, and comparison to standards of 1-hexanol and 2-hexanol using GC-MS revealed that only 1-hexanol had formed. This confirms that the formation of labeled alcohols by the exchange reaction described above involves a S_N2 mechanism, as illustrated in Schemes 6 and 7. (Supporting Information Figures 2 and 3).

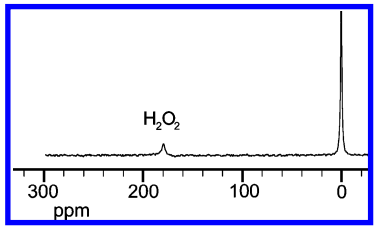

Figure 4. ^{17}O NMR spectrum of labeled hydrogen peroxide.

Effects of ^{17}O on the ^{1}H and ^{13}C Chemical Shifts in Hexanol and Camphor. *1-Hexanol.* The proton NMR coupling of the methylene protons at C-1 (labeled H_1 in Chart 1) was examined, and a small isotope-induced shift (+0.005 ppm) was found. In addition, for nonlabeled hexanol, the CH_2 protons showed a triplet (Figure 5a) due to coupling with the adjacent CH_2 protons whereas in the ^{17}O-labeled hexanol, a doublet of triplets (dt) was observed which mimics a quartet (Figure 5b). We propose this additional splitting in labeled hexanol results from coupling with the exchangeable ^{17}OH proton. Because $^3J_{H1\text{-}Hex}$ (5.5 Hz) is approximately equal to $^3J_{H1-H2}$ (6.6 Hz), the resulting dt is a multiplet that closely resembles a quartet. In the nonlabeled 1-hexanol this coupling to the hydroxyl proton was not seen, probably because of a much more rapid hydrogen exchange rate in the ^{16}OH group than in the ^{17}OH. When the hydrogen exchange rate is sufficiently slow for coupling to occur, one can occasionally observe coupling between an exchangeable OH proton and a hydrogen on a neighboring atom.

The $^2J_{O-H}$ coupling in 1-^{17}O-hexanol could not be resolved, because the chemical shift of the hydroxyl proton was close to that of the methylene protons (H_3, H_4, and H_5), so that these protons (H_3, H_4, H_5, and OH) appeared together as a multiplet (1.26−1.38 ppm) (Supporting Information Figures S4 and S6). It has been suggested for water (and we have observed this too, see below, Figure 6a) that the $^2J_{O-H}$ coupling is difficult to observe in the ^{1}H spectra because of the short lifetimes of the six ^{17}O states.[44]

The ^{13}C NMR spectra of 1-hexanol suggest that C_1, C_2 are deshielded in the labeled hexanol (Chart 1) (Supporting Information Figure S7) when compared to commercial 1-hexanol (Supporting Information Figure S5). The remaining carbon or hydrogen atoms showed no significant change in their chemical shifts.

Camphor. The ^{1}H NMR spectrum of labeled camphor (Chart 2) (Supporting Information Figure S12) suggests that protons are slightly deshielded (shown circled) in ^{17}O-camphor compared to the ^{16}O compound (Supporting Information Figure S10). The ^{13}C NMR chemical shift difference of the labeled (Supporting Information Figure S13) and nonlabeled camphors (Supporting Information Figure S11) suggest that the C_2 carbon is shielded (shown in bold) in the labeled camphor and the rest of the carbons were more deshielded in ^{17}O-labeled camphor than in the nonlabeled compound. (Table 2). Qin et al. have reported the effects on ^{13}C and ^{17}O chemical shifts with respect to the

(42) Chamberlin, A. R.; Stemke, J. E.; Bond, F. T. *J. Org. Chem.* **1978**, *43*, 147–154.
(43) Casny, M.; Rehder, D.; Schmidt, H.; Vilter, H.; Conte, V. *J. Inorg. Biochem.* **2000**, *80*, 157–160.
(44) de Graaf, R. A.; Brown, P. B.; Rothman, D. L.; Behar, K. L. *J. Magn. Reson.* **2008**, *193*, 63–67.

Scheme 7. Reaction of Labeled Camphor in Hexanol with ^{17}O-Enriched Water

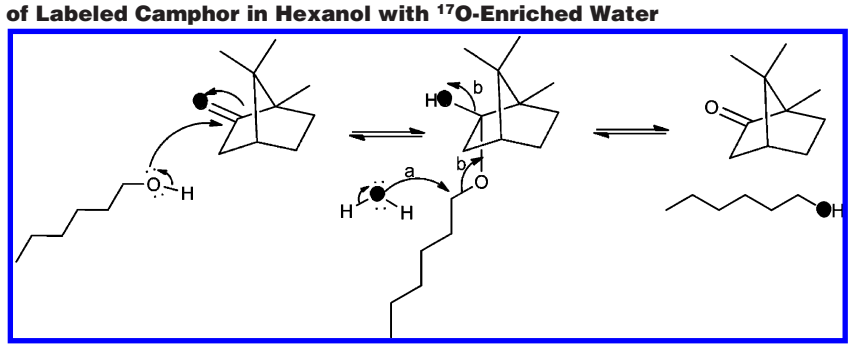

Chart 1

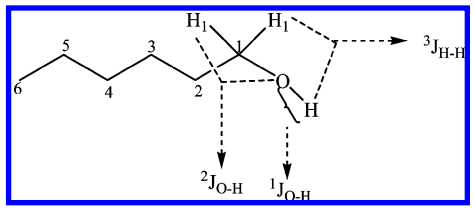

size of alkyl substituents in (1-adamantyl) alkyl ketones. Their results indicate that as the size of the alkyl substituent increases, upfield chemical shifts in ^{13}C NMR and downfield shifts in the ^{17}O NMR of the carbonyl group were observed.[45]

The ^{1}H NMR data of the ^{17}O labeled compounds (camphor, hexanol, and HMDS) are in the Supporting Information: (Supporting Information Figures S4−S13). Comparison of ^{1}H and ^{13}C NMR data for the ^{17}O-labeled compounds with the nonlabeled compounds showed subtle effects of the ^{17}O on both ^{1}H and ^{13}C chemical shifts near the ^{17}O (see below, Table 2).

^{1}H NMR Spectra of $H_2{}^{17}O$ and Determination of Coupling Constant (J_{OH}) of $H_2{}^{17}O$. Attempts to use ^{1}H NMR to independently quantify the percentage of ^{17}O isotopic labeling in the enriched water were unsuccessful, as we could not resolve a clear ^{1}H−^{17}O sextet from the ^{1}H−^{16}O singlet in the ^{1}H NMR spectra of dilute mixtures of enriched water in $CDCl_3$ or CD_3CN. This is most likely because the relaxation rate of the ^{17}O is faster than ^{1}H, and this gives an underestimate of the coupling constant $^{1}J_{O-H}$ in ^{1}H NMR.[46] Conversely, it was possible to observe the $^{1}J_{O-H}$ coupling in $H_2{}^{17}O$ using ^{17}O NMR. The ^{17}O NMR spectrum of a sample of ∼90% enriched $H_2{}^{17}O$ in CD_3CN which had been carefully shimmed manually in order to obtain the best possible resolution showed a well-resolved triplet with a coupling constant of 80 Hz (Figure 6a), in agreement with the literature.[47] This triplet could not be observed in $CDCl_3$, and the possible reason could be due to rapid exchange of the OH protons in $CDCl_3$. Previous ^{17}O NMR literature has also reported the observation of $^{1}J_{O-H}$ coupling for $H_2{}^{17}O$ dissolved in CD_3CN,[47] CH_3COCH_3,[48] CCl_4,[49] at 273 K.

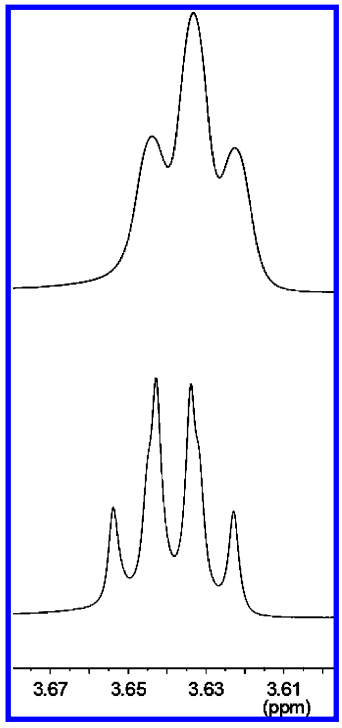

Figure 5. The coupling pattern of methylene (CH_2) protons attached to C-1 in hexanol. (a) Triplet observed for commercial hexanol. (b) Doublet of triplets observed in labeled hexanol.

The ^{1}H NMR spectrum of $H_2{}^{17}O$ in $CDCl_3$ revealed that the chemical shift of the protons was 1.57 ppm (Supporting Information Figure S14), 0.03 ppm downfield from the chemical shift of nonlabeled water, 1.54 ppm (Supporting Information Figure S15). We also checked the ^{1}H NMR chemical shifts of 25%, 50%, and 75% labeled water samples in $CDCl_3$ (Supporting Information Figure S16) and have observed a linear relationship between the chemical shift and percentage of ^{17}O labeling. (Figure 6b). This phenomenon could be used, in conjunction with GC-MS of water derivatives, to establish the percentage of enrichment of water samples, especially during the enrichment procedure.

GC-MS Retention Times (isotope fractionation). The introduction of isotopes often changes the retention of the material on GC columns, either to a shorter or longer retention time. For example, ^{2}H-labeled compounds tend to partition to shorter retention times on nonpolar GC columns.[50] Similarly, the use of $H_2{}^{18}O$ to study the metabolic pathways and mass shifts due to isotope effects have been reported previously.[51]

(45) Qin, X. R.; Ishizuka, Y.; Lomas, J. S.; Tezuka, T.; Nakanishi, H. *Magn. Reson. Chem.* **2002**, *40*, 595–598.
(46) Pople, J. A. *Mol. Phys.* **1958**, *1*, 168–174.
(47) Halle, B.; Karlstrom, G. *J. Chem. Soc., Faraday Trans. 2* **1983**, *79*, 1031–1046.
(48) Rabideau, S. W.; Hecht, H. G. *J. Chem. Phys.* **1967**, *47*, 544.
(49) Mateescu, G. D.; Benedikt, G. M. *J. Am. Chem. Soc.* **1979**, *101*, 3959–3960.
(50) Attygalle, A. B.; Blankespoor, C. L.; Eisner, T.; Meinwald, J. *Proc. Natl. Acad. Sci. U.S.A.* **1994**, *91*, 12790–12793.
(51) Matsunaga, T.; Kishi, N.; Higuchi, S.; Watanabe, K.; Ohshima, T.; Yamamoto, I. *Drug Metab. Dispos.* **2000**, *28*, 1291–1296.

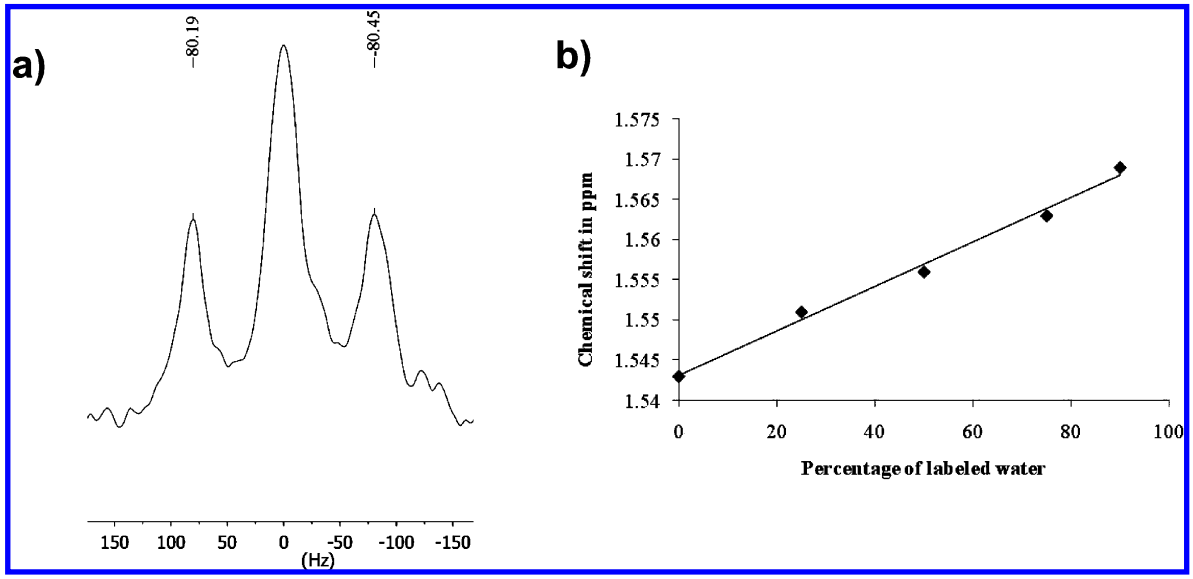

Figure 6. (a) ^{17}O NMR spectrum of 1 μL of 90% enriched water dissolved in CD_3CN (540 μL) acquired at 67.8 MHz without ^1H decoupling using 5 mm TBO probe, spectral width 800 ppm, 18935 scans, 0.2 s recycle delay, $T = 298$ K). (b) Chemical shifts of varying proportions of ^{17}O and ^{16}O water in $CDCl_3$.

Chart 2

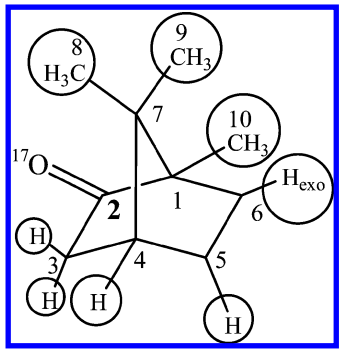

Table 2. The Effect of ^{17}O Shielding Cone on the ^{13}C and ^1H Chemical Shifts in Camphor

assignment[a]	$\Delta\delta^b$ ^{13}C (ppm)	$\Delta\delta^b$ ^1H (ppm)
1	+0.01	–
2	−0.02	–
3	+0.02	exo (∼+0.01) endo (∼+0.01)
4	+0.02	∼+0.01
5	+0.02	∼+0.01
6	+0.02	∼+0.01
7	+0.02	–
8	+0.02	∼+0.01
9	+0.02	∼+0.01
10	+0.02	∼+0.01

[a] Refers to the position of carbon or hydrogen atom as numbered in Chart 2. [b] Chemical shift differences observed in the ^{13}C NMR and ^1H NMR spectra for labeled and unlabeled camphor. $\Delta\delta < 0$ indicates that the signal is shielded in labeled relative to nonlabeled camphor while $\Delta\delta > 0$ means the signal is deshielded.

The nonlabeled (mainly ^{16}O) hexanol (Sigma) derivatized by BSTFA had a retention time of 10.32 min, and ^{17}O-labeled hexanol derivatized by BSTFA had a longer retention time 10.515 min. (Supporting Information Figure S17). The ^{17}O HMDS had a retention time of 7.010 min and the ^{16}O HMDS had a retention time of 6.865 min. (Supporting Information Figure S18). Thus, for both TMS derivatives, the retention time of the labeled compound was longer than that of the ^{16}O compounds. In the case of 1-hexanol, the isotope fractionation was sufficient to get baseline separation of the labeled and nonlabeled pair.

GC-MS Fragmentation Pattern Analysis. The nonlabeled 1-hexyl trimethylsilyl (TMS) ether showed an M − 1 ion at m/z 173 in its mass spectrum (Supporting Information Figure S17) whereas ^{17}O-labeled 1-hexyl-TMS ether showed the molecular ion $M^{\cdot+}$ at m/z 175. Presumably an isotope effect in the ^{17}O-labeled compound prevented the loss of a hydrogen atom (Scheme 3), as seen abundantly for the nonlabeled compound. HMDS fragmented by the loss of methane to fragment ions m/z 146 in the case of deionized water ($H_2{}^{16}O$), m/z 147 in the case of $H_2{}^{17}O$ and m/z 148 in the case of $H_2{}^{18}O$ (Scheme 3). The mass spectrum of the TMS ether of $H_2{}^{17}O$ was (EI): m/z (% of base peak) 147 (100), 145 (12.5), 135 (25), 134 (45), 131 (35) (Supporting Information Figure S18).

The GC-MS isotope fractionation and fragmentation analysis of nonlabeled and ^{17}O labeled camphors, MS-MS data of nonlabeled and ^{17}O labeled camphors, and ^{16}O- and ^{17}O-1-hexanols is included in the Supporting Information.

SUPPORTING INFORMATION AVAILABLE

The experimental details, ^{1}H, ^{13}C NMR, and the mass spectra of camphor, hexanol, and HMDS. This material is available free of charge via the Internet at http://pubs.acs.org.

Received for review September 1, 2010. Accepted November 15, 2010.

AC1022887

SUPPORTING INFORMATION

Enrichment of $H_2{}^{17}O$ from Tap Water and Characterization of the Enriched Water and Several ^{17}O-Labelled Compounds

Brinda Prasad[a], Andrew R. Lewis[a] and Erika Plettner[a]*

[a]Department of Chemistry, Simon Fraser University, 8888 University Drive, Burnaby, BC, V5A1S6, Canada.

***Corresponding author: Tel: (+1)-778-782-3586; fax: (+1)-778-782-3765.**

Email address: plettner@sfu.ca

Table of Contents.

Experimental details:

1) Characterization of the enriched water by its density, refractive index, ^{1}H and ^{17}O NMR.

a) Density and refractive index: The density of the water fraction having a boiling point of 99 °C was determined at room temperature (21 °C), using a calibrated pipettor and a balance. A known volume of the water was weighed on an analytical balance. A sample of normal deionized water (prepared by reverse osmosis, Barnstead/Thermolyne Nanopure Infinity ultrapure water system) was used as a density reference. The refractive index was determined at a temperature of 24.5 °C at λ=589 nm using a Leica Mark II Abbe refractometer. Again, deionized water was used as a reference.

b) ^{1}H, ^{13}C and ^{17}O NMR NMR settings:

NMR spectra were run on a Bruker AVANCE II 600 MHz digital NMR spectrometer equipped with a Bruker 5 mm BBO probe. The ^{17}O NMR spectra of cyclohexanone and ethanol were run on a Bruker 500 MHz NMR spectrometer equipped with a Bruker 5 mm TBO probe. In these probes the ^{1}H channel was on the outer coil and the broad-banded inner coil used tuned to ^{17}O (81.3 or 67.8 MHz) or ^{13}C (150 MHz). The sample temperature was maintained at 298 K (Bruker BVT 3000 temperature controller with Bruker BCU-05 cooler unit). For the acquisition of the ^{17}O spectra, most samples were required to be run as unaltered reaction mixtures so in order to prevent ^{1}H-^{2}H exchanges occurring, deuterated solvents were not added. For this reason many of the NMR spectra were acquired without the ^{2}H lock engaged and the field sweep off. The lack of deuterated solvent meant sample shimming had to be performed by manually adjusting currents in the various room-temperature shim coils to optimize the ^{1}H spectrum of the sample, which was observed in real-time (continuous single scan mode). Corrections for magnetic drift (< 1 Hz / h) occurring due to the unlocked operation mode were not important because the ^{17}O peak widths were large (> 50 Hz) and spectral acquisition typically only required 1-2 hours. In some cases a co-axial capillary containing $CDCl_3$ was inserted and used for ^{2}H locking, ^{1}H and ^{13}C chemical shift referencing purposes. In other cases a co-axial capillary containing $H_2{}^{17}O$ was inserted to provide ^{17}O chemical shift referencing. ^{17}O chemical shifts were referenced to pure $H_2{}^{17}O$ (0 ppm). ^{1}H and ^{13}C chemical shift scales were referenced using the chemical shifts of $CDCl_3$ (7.26 and 77.16 ppm

respectively). ^{1}H decoupling was achieved using WALTZ-16 composite pulse decoupling with the ^{1}H transmitter set to 4 ppm. Acquisition parameters for ^{17}O{^{1}H} NMR spectra: spectral width 600 ppm, transmitter set to 0, 75 or 300 ppm, 90-degree pulse, 0.2 s recycle delay, 16-60000 scans with 8192 complex data points were accumulated and Fourier transformed using two-fold zero-filling and 30-50 Hz exponential line broadening. Acquisition parameters for ^{1}H NMR spectra: spectral width 16 ppm, transmitter set to 3 ppm, 30-degree pulse, 1 s recycle delay, 16 scans with 64k complex data points were accumulated and Fourier transformed using two-fold zero-filling and 0.2 Hz exponential line broadening. Acquisition parameters for ^{13}C{^{1}H} NMR spectra: spectral width 260 ppm, transmitter set to 110 ppm, 30-degree pulse, 2 s recycle delay, 512 scans with 128k complex data points were accumulated and Fourier transformed using two-fold zero-filling and 1 Hz exponential line broadening.

2. NMR details of hexanol (labeled and non-labeled), camphor (labeled and non-labeled).

a) Hexanol:

^{1}H NMR (Supp. Info. Fig. **S4**) of 10 µL of 1-hexanol (Sigma) in 580 µL of $CDCl_3$ + 10 µL of water (600 MHz, $CDCl_3$): δ 7.26 ($CDCl_3$), 3.63 (t, 2H, J = 6 Hz) H_1, 1.56 (quintet, 2H, J = 6 Hz) H_2, 1.28-1.37 (m, 8H) H_3, H_4, H_5 and OH, 0.89 (t, J = 6 Hz, 3H) H_6. ^{13}C NMR (Supp. Info. Fig. **S5**) of 10 µL of hexanol (Sigma) in 580 µL of $CDCl_3$ + 10 µL of water (151 MHz, $CDCl_3$) δ 77.16 ($CDCl_3$) [1], 63.22, 32.92, 31.78, 25.56, 22.76, 14.13. ^{1}H NMR (Supp. Info. Fig. **S6**) of 10 µL of labelled hexanol reaction mixture in 580 µL of $CDCl_3$ (600 MHz, $CDCl_3$) δ 7.26 ($CDCl_3$), 3.64 (q, 2H, J= 6 Hz) H_1, 1.57 (quintet, 2H, J = 6 Hz), 1.27-1.38 (m, 7H) H_3, H_4, H_5 and OH, 0.89 (t, 3H, J = 6 Hz). ^{13}C NMR (Supp. Info. Fig. **S7**) of 10 µL of labelled hexanol reaction mixture in 580 µL of $CDCl_3$ (151 MHz, $CDCl_3$): δ 77.16, 63.24, 32.94, 31.78, 25.57, 22.76, 14.14.

b) camphor:

^{1}H NMR (Supp. Info. Fig. **S10**) of 7 mg of camphor in 590 µL of $CDCl_3$ and 10 µL of normal water (600 MHz, $CDCl_3$) δ 7.26, 2.31-2.36 (m, 1H) H_3 exo, 2.07 (t, 1H, J=4.36 Hz) H_4, 1.91-1.97 (m, 1H) H_5, 1.81-1.84 (d, 1H, J=18.25 Hz) H_5 endo, 1.65-1.69 (m, 1H) H_6 exo, 1.37-1.42 (m, 1H) H_6 endo, 1.30-1.35 (m, 2H) H_5 exo, 0.95 (s, 3H) H_{10}, 0.90 (s, 3H) H_9, 0.82 (s, 3H) H_8. ^{1}H decoupled ^{13}C NMR (Supp. Info. Fig. **S11**) of 7 mg of camphor in

590 µL of $CDCl_3$ and 10 µL of normal water (locked on $CDCl_3$): δ 219.76 (C_2), 77.16, 57.84 (C_1), 46.93 (C_7), 43.45 (C_3), 43.24 (C_4), 30.09 (C_6), 27.20 (C_5), 19.91 (C_{10}), 19.28 (C_9), 9.36 (C_8).

^{1}H NMR (Supp. Info. Fig. **S12**) of 7 mg of ^{17}O camphor in 590 µL of $CDCl_3$ and 10 µL of labelled water (600 MHz, $CDCl_3$) δ 7.27, 2.32-2.37 (m, 1H) H_3 exo, 2.08 (t, 1H, J=4.26 Hz) H_4, 1.92-1.97 (m, 1H) H_5, 1.82-1.85 (d, 1H, J=18.12 Hz) H_3 endo, 1.65-1.71 (m, 1H) H_6 exo, 1.39-1.43 (m, 1H) H_6 endo, 1.32-1.36 (m, 1H) H_5 exo, 0.95 (s, 3H), H_{10}, 0.91 (s, 3H), H_9, 0.83 (s, 3H) H_8. ^{1}H decoupled ^{13}C NMR of 7 mg of ^{17}O camphor in 590 µL of $CDCl_3$ and 10 µL of ^{17}O-labelled water, locked on $CDCl_3$ (Supp. Info. Fig. **S13**): δ 219.74 (C_2), 77.16, 57.85 (C_1), 46.94 (C_7), 43.47 (C_3), 43.26 (C_4), 30.10 (C_6), 27.21 (C_5), 19.92 (C_{10}), 19.30(C_9), 9.38 (C_8).

C) Oxygen exchange of camphor. The exchange of the camphor oxygen was detected indirectly in the ^{1}H NMR spectrum. For this, 7 mg of camphor was dissolved in 580 µL of $CDCl_3$ and exchanged with 10 µL of $H_2{}^{17}O$ and a ^{1}H NMR was run after 2 hrs. The multiplet at 1.65-1.70 ppm was due to the proton on the 6th carbon (exo) position and a singlet at 1.59 ppm due to $H_2{}^{17}O$ was observed. (Supp. Info. Fig S12 (c)). The sample was allowed to react overnight and a ^{1}H NMR was run for a similar number of scans the next day. The results shown in Figure 4b illustrates that the peak at 1.59 ppm disappeared and multiplet was detected at 1.65-1.70 ppm (Supp. Info. Fig S12 (d)). This suggests that the camphor oxygen exchange at C-2 affects the chemical shift of the H_6 exo proton.

3) Gas Chromatography-Mass Spectrometry (GC-MS) column oven settings and configuration.

a) Column oven settings: The column oven was programmed as follows: 45 °C (0.5 min), 7 °C min^{-1} to 120 °C (1 min), 50 °C min^{-1} to 260 °C (3 min). The mass spectrometer was programmed for ion collection between m/z 90 and 180 amu, emission current 30 µA, trap temperature 170 °C and transfer line 250 °C were applied for MS settings. For sensitivity measurements, electron impact (EI) spectra were obtained with ion storage (SIS mode) m/z 150-180 amu in those cases when 1-hexanol was derivatized with BSTFA. MS/MS spectra were obtained for parent ion masses 173, 174 and 175 in the case of labeled and non-labeled hexanols. For MS/MS spectra, the ejection amplitude was set to be 20 V, ionisation storage level was set up to 48 m/z.

b) GC-MS fragmentation and mass spectral analysis of camphor:

The ^{17}O exchanged camphor, in contrast to ^{17}O-labeled hexanol and ^{17}O HMDS had a shorter retention time of 10.051 min when compared to the non-labeled camphor (10.338 min) (Supp. Info. Fig S19).

The ^{17}O exchanged camphor, had a mass spectrum (EI): m/z (% of base peak) 153 ($M^{+\cdot}$, 6), 152 (8), 137 (M-18, 7), 108 (66), 95 (100). The molecular ion and the M-1 ion are usually small, and do not provide a clear indication of labeling in ^{17}O camphor. The fragment ion that corresponds to the loss of 16 amu from camphor (m/z 136 in non-labeled camphor) clearly showed labeling, whereas the other two major fragment ions, often seen for monoterpenes, did not label. This suggests that m/z 136 (in non-labeled camphor) contains oxygen, whereas m/z 108 and m/z 95 do not contain oxygen. (Supp. Info. Fig S19).

c) MS-MS analysis for hexanol. An ion with m/z 173 was seen in both labeled and non-labeled 1-hexanols. To check if this ion of m/z 173 differed in labeled and non-labeled hexanols, MS/MS was performed for the hexanols taking 173, 174 and 175 as the parent ions. (Supp. Info. Figs 20, 21 and 22) (Table S1).

d) MS-MS analysis for camphor. The labeled and the non-labeled camphor showed m/z 153 ($M^{\cdot+}$ of labeled, M+1 of non-labeled) and 152 ($M^{\cdot+}$ of non-labeled, M-1 of labeled) ions in their mass spectra. To verify whether 152 (M-1) ion and 153 ($M^{+\cdot}$) in the labeled camphor has a different structure compared to the 152 ($M^{\cdot+}$) of non-labeled camphor, MS-MS of camphor taking 152 and 153 as the parent ions was performed. (Supp. Info. Fig. No. 23 and 24). The m/z 154 ion (Supp. Info. Fig. 25) fragmented into 153 ($M^{\cdot+}$) and 152 (M-1) in labeled camphor, whereas in non-labeled camphor it fragmented to 153 (M+1) only. This confirms that 152, 153 and 154 ions have a different structure in labeled and non-labeled camphors (refer Table S1 for the complete list of ions).

Table S1. MS-MS analysis of hexanols (labeled and non-labeled) and camphor (labeled and non-labeled)

Compound	Parent ion (m/z)	Assignment of parent ion	Daughter ions in MS/MS (m/z)
^{16}O 1-hexanol	173	M-1	171.5, 173, 174
	174	$M^{\cdot+}$	172
	175	M+1	174, 171.5
^{17}O 1-hexanol	173	M-2	173, 174
	174	M-1	172, 174
	175	$M^{\cdot+}$	175
^{16}O camphor	152	$M^{\cdot+}$	153
	153	M+1	137, 136
	154	M+2	152
^{17}O camphor	152	M-1	152, 153, 154
	153	$M^{\cdot+}$	151, 152, 153
	154	M+1	151, 152

4. Quantitation of hydrogen peroxide. Hydrogen peroxide was detected using two colorimetric assays [2, 3]: the first tests the reducing ability of H_2O_2 and the second one tests the oxidising ability. To test the reducing ability of the H_2O_2 solution, 100 µL of the electrolysed solution was treated with 200 µL of 3% w/v trichloroacetic acid (TCA) and left at 4 °C for 20 minutes. Further treatment with 10 mM $KMnO_4$ resulted in the decolorisation of the permanganate.

$$2MnO_4^- + 6H^+ + 5H_2O_2 \longrightarrow 2Mn^{2+} + 8H_2O + 5O_2$$

To test for the oxidising abilities of the hydrogen peroxide, 500 µL of the electrolysed water was treated with 1000 µL of 3% w/v trichloroacetic acid (TCA) and left at 4 °C for 20 minutes. Further treatment with 250 µL of ferrous ammonium sulphate ($Fe(NH_4)_2SO_4$) and 125 µL of potassium thiocyanate (KSCN) resulted in the formation of a reddish brown complex ($Fe(SCN)_3$):

$$3Fe^{2+}(aq) + H_2O_2 + 2\ H^+(aq) \longrightarrow 2\ Fe^{3+}(aq) + 2H_2O(l)$$

The absorbance of the Fe^{3+} (as $Fe(SCN)_3$ complex) was monitored at 480 nm on a UV-Visible spectrophotometer (Hach DR/4000U). A calibration curve for hydrogen peroxide concentrations was prepared using a series of solutions of known concentrations. The concentration of hydrogen peroxide obtained by electrolysis was found to be 0.1 mM using both methods.

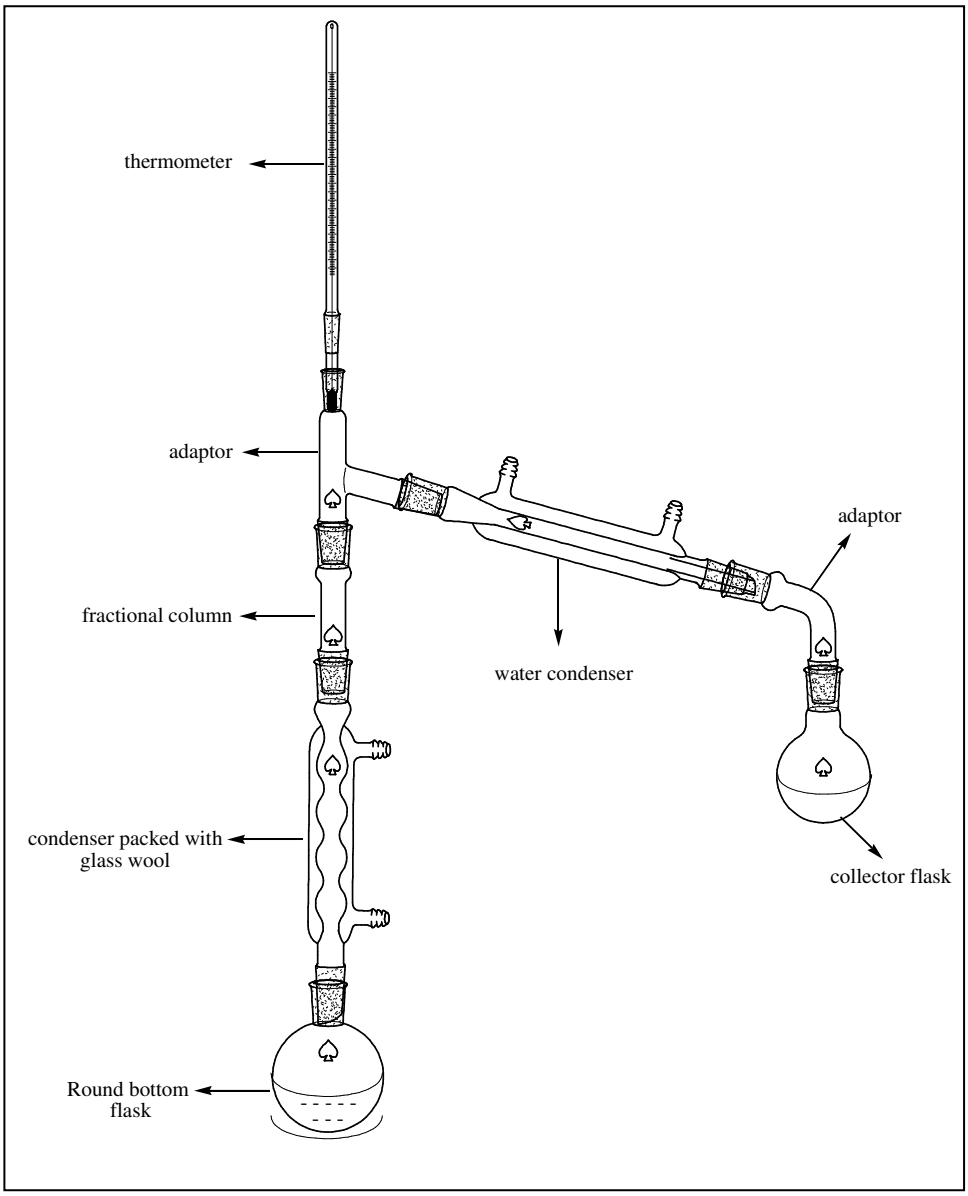

Figure S1. Enrichment of $H_2{}^{17}O$ from tap water by fractional distillation.

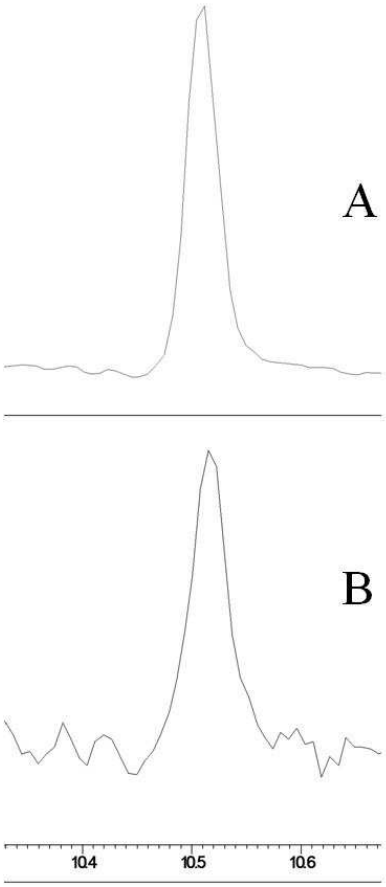

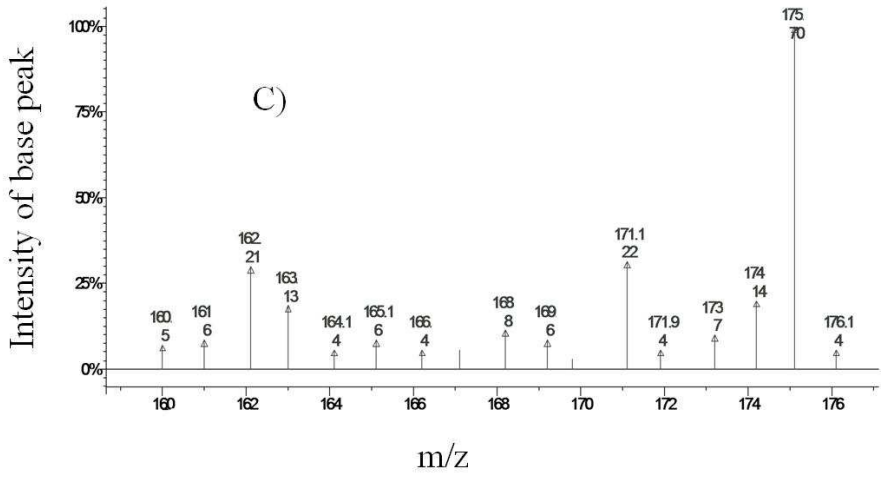

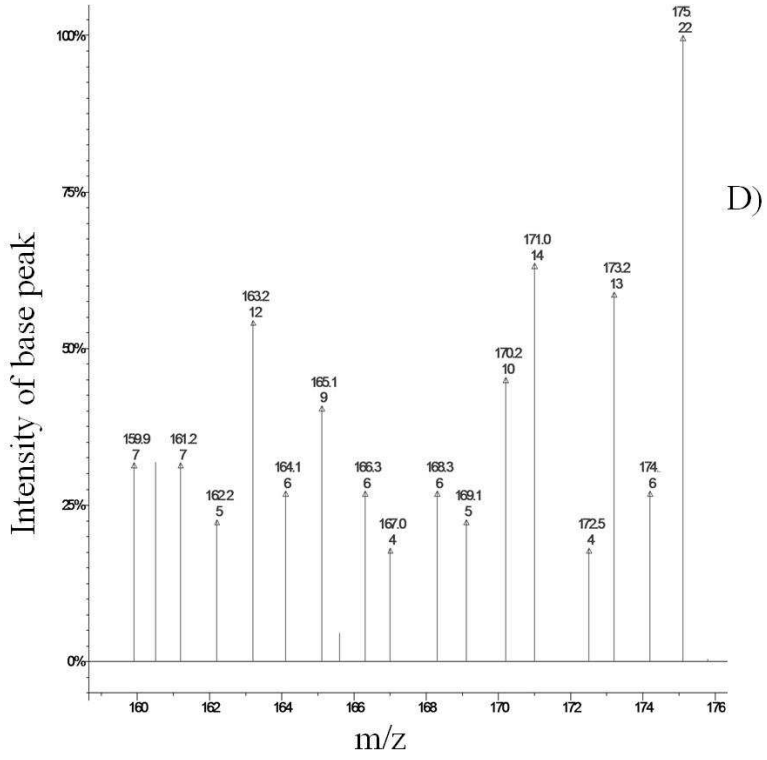

Figure S2. A) GC-MS trace (ions displayed) of ^{17}O-labelled 1-hexanol. B) GC-MS trace (ions displayed) of ^{17}O-labelled hexanol synthesized by the nucleophilic attack of hexanol and ^{17}O-labelled water (by reaction of camphor +hexanol + $H_2{}^{17}O$; see text for more details). C) Mass spectrum of ^{17}O-labelled 1-hexanol. D) Mass spectrum of ^{17}O-labelled 1-hexanol formed by the S_N2 reaction

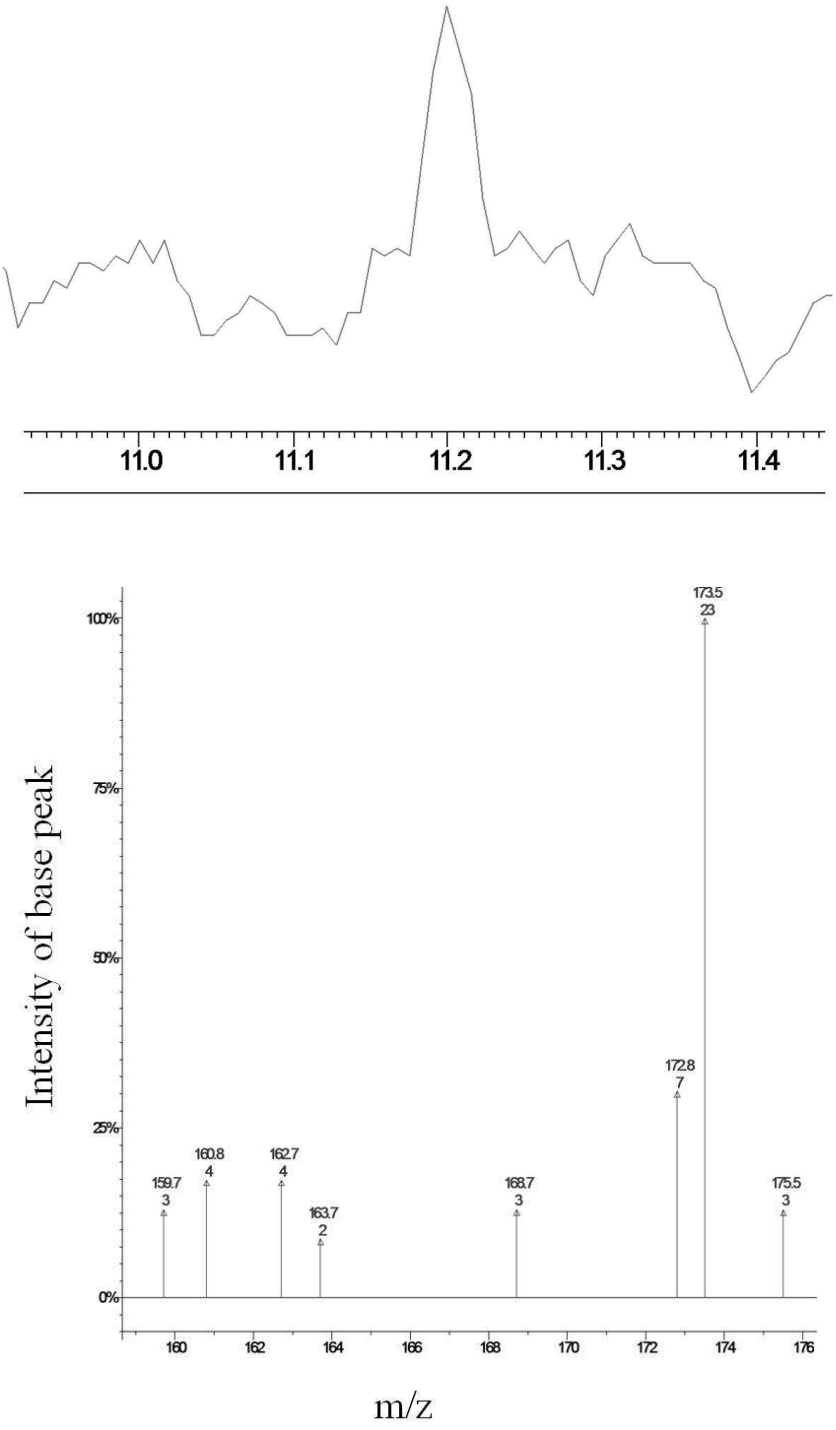

Figure S3: GC-MS trace (ions displayed) and Mass spectrum of 2-hexanol

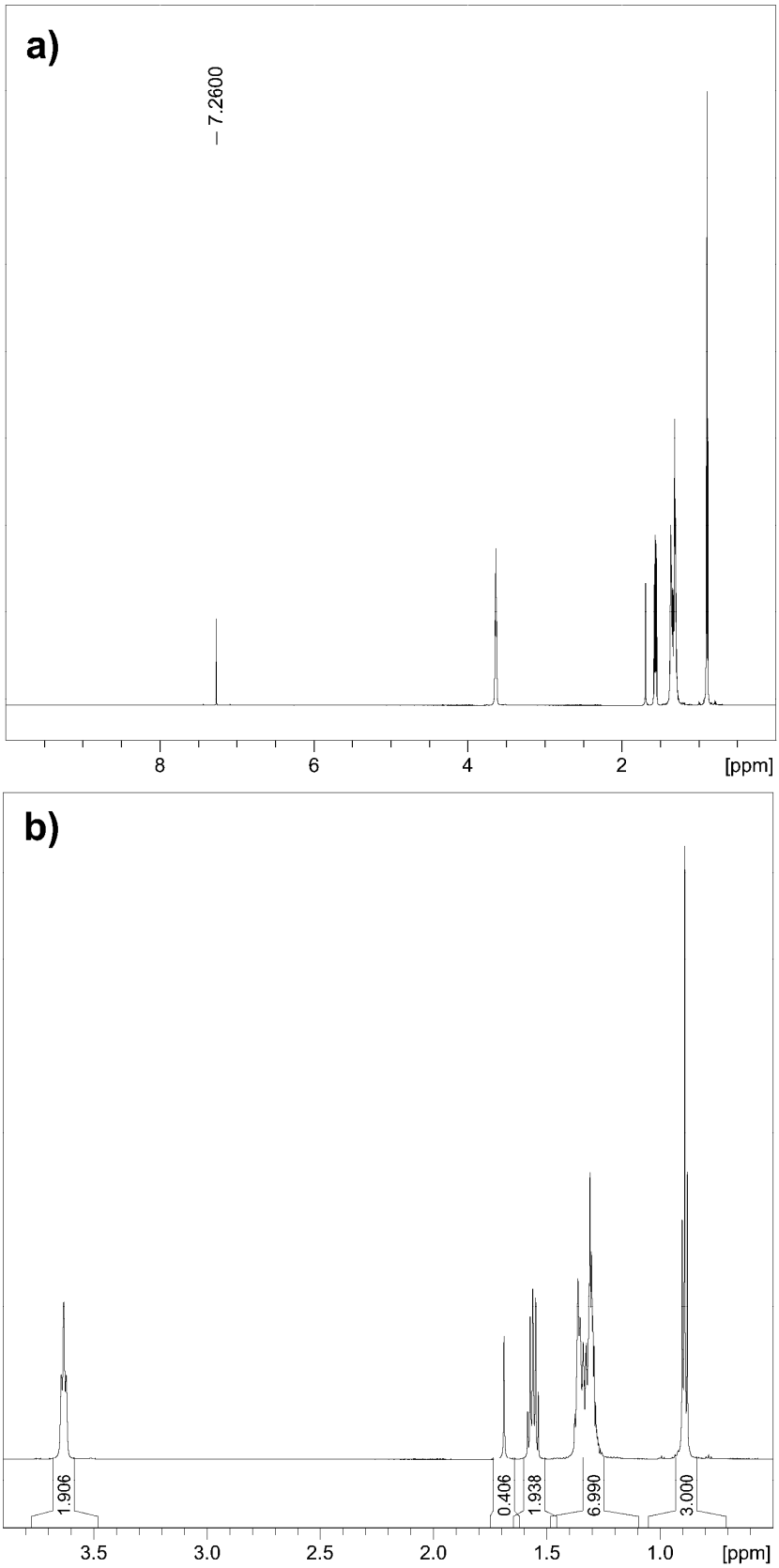

Figure S4. ^{1}H NMR spectrum of 10 µL of unlabelled hexanol (SIGMA) in 580 µL of $CDCl_3$ and 10 µL of unlabelled water. 90 degree ^{1}H pulse, spectral width 16 ppm, 16 scans, 1 s recycle delay, 65536 complex data points, acquisition time 3.40 s, ^{1}H transmitter set to 3 ppm, 2 x zero-filled with 0.1 Hz line-broadening applied. **a)** 0 - 10 ppm region, **b)** expansion of 0.5 - 3.9 ppm region.

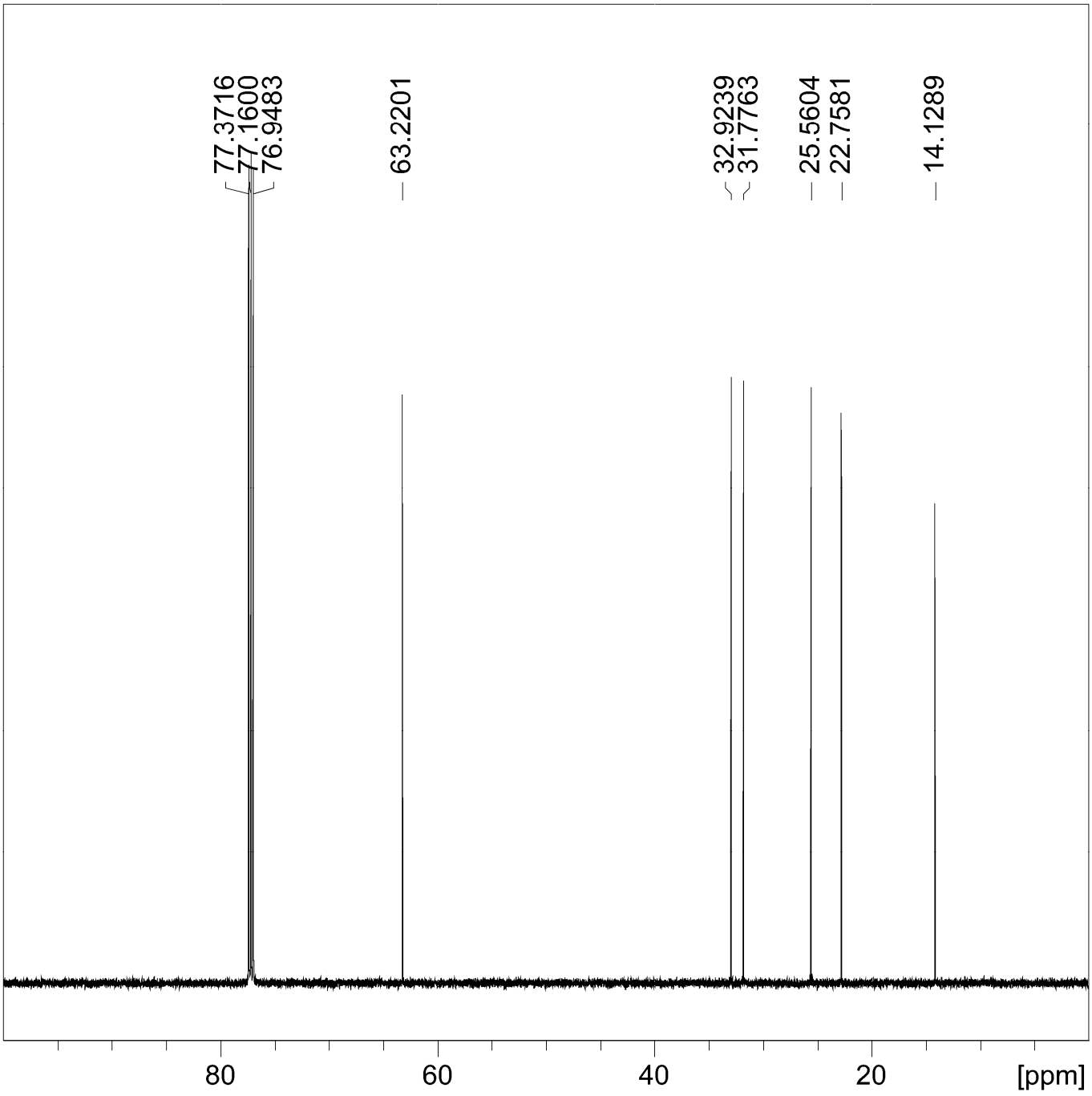

Figure S5. $^{13}C\{^{1}H\}$ NMR spectrum of 10 µL of unlabelled hexanol (SIGMA) in 580 µL of $CDCl_3$ and 10 µL of unlabelled water. 30 degree ^{13}C pulse with power-gated WALTZ-16 ^{1}H composite pulse decoupling, spectral width 260 ppm, 256 scans, 4 dummy scans, 2 s recycle delay, 131072 complex data points, acquisition time 1.68 s, ^{13}C transmitter set to 110 ppm, ^{1}H transmitter set to 4 ppm, 2 x zero-filled with 0.3 Hz line-broadening applied.

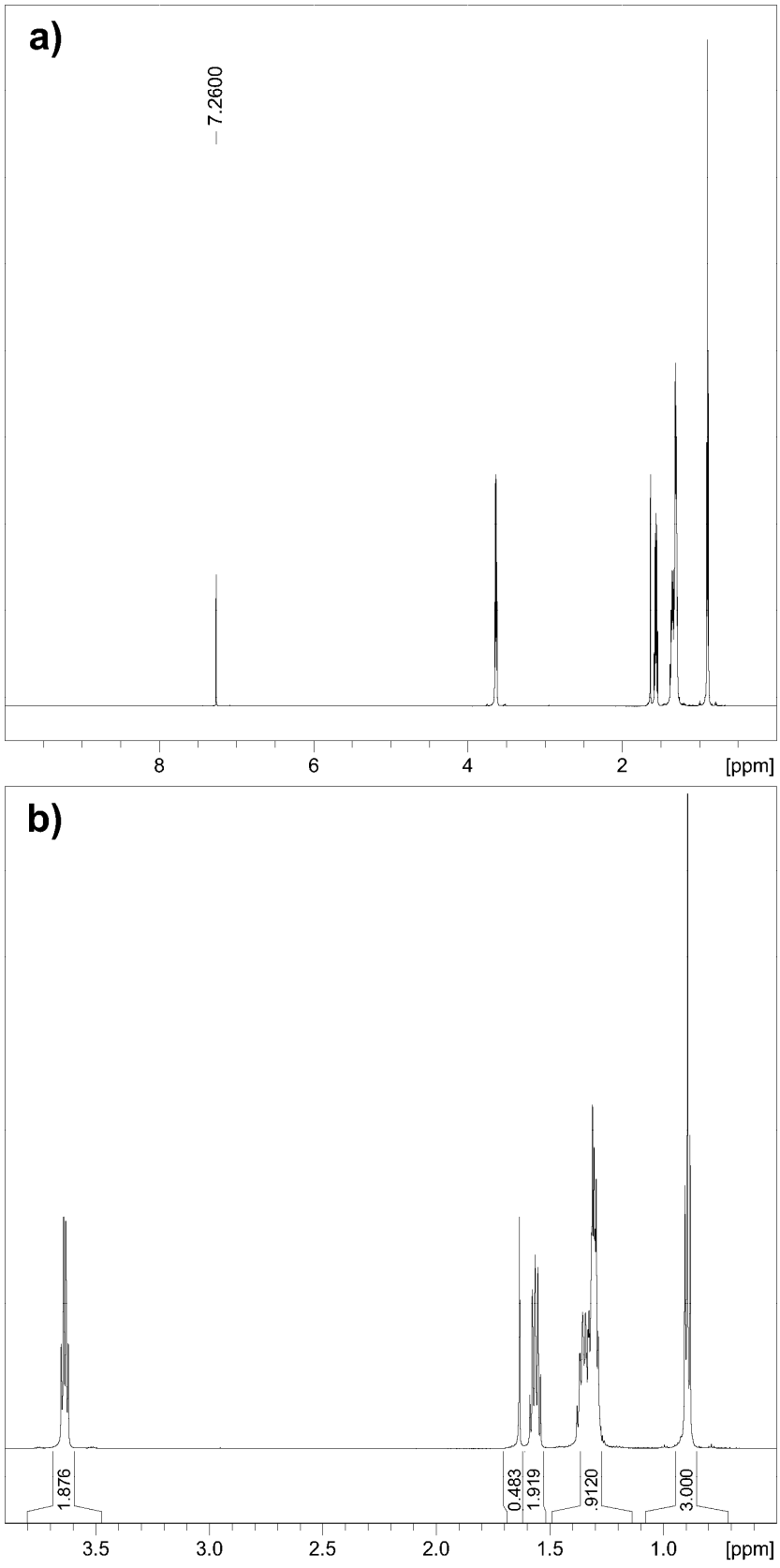

Figure S6. ^{1}H NMR spectrum of 10 µL of aqueous ^{17}O-labelled hexanol mixture in 590 µL of $CDCl_3$. 90 degree ^{1}H pulse, spectral width 16 ppm, 16 scans, 1 s recycle delay, 65536 complex data points, acquisition time 3.40 s, ^{1}H transmitter set to 3 ppm, 2 x zero-filled with 0.1 Hz line-broadening applied. **a**) 0 - 10 ppm region, **b)** expansion of 0.5 - 3.9 ppm region.

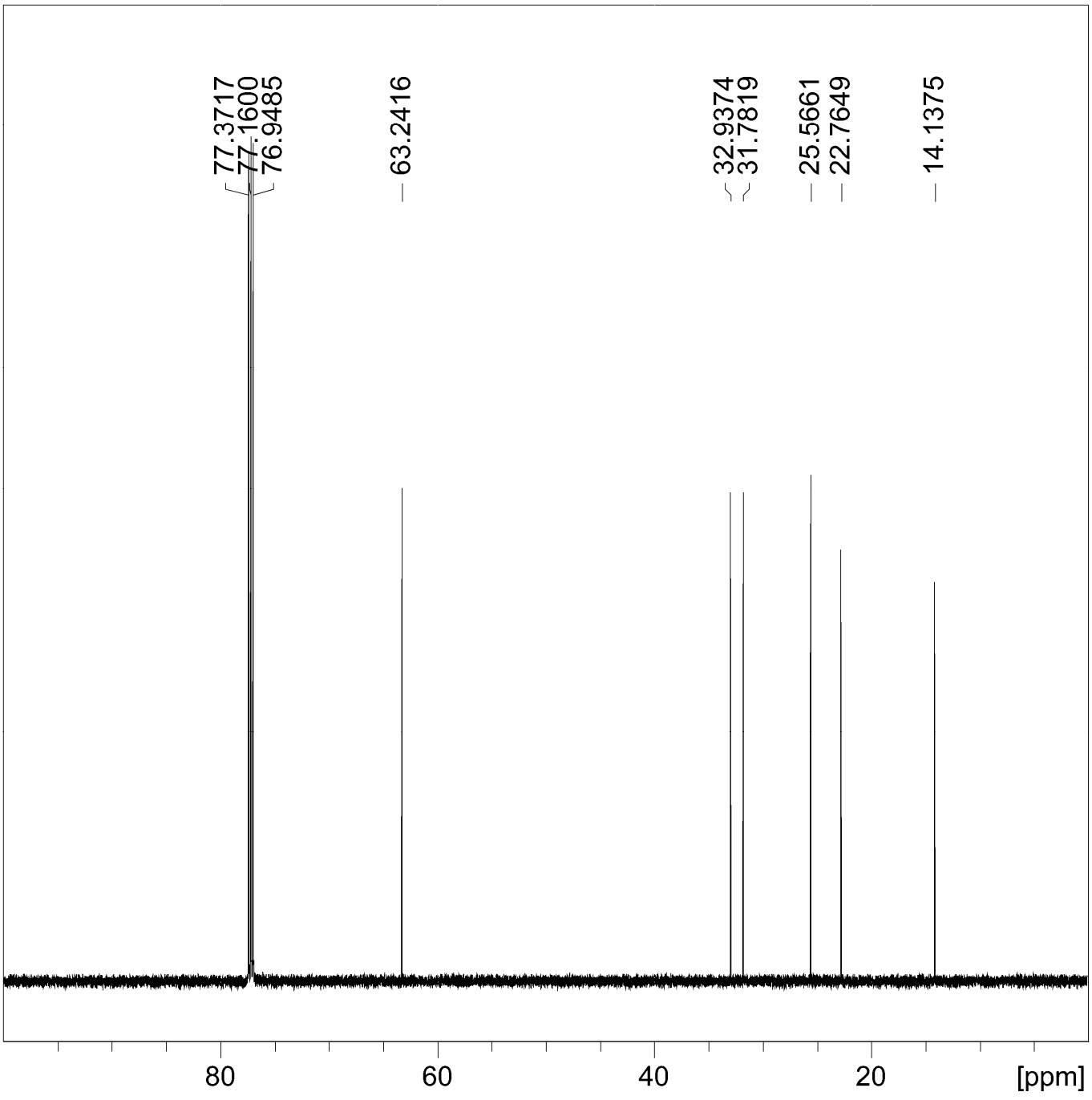

Figure S7. $^{13}C\{^{1}H\}$ NMR spectrum of 10 µL of aqueous ^{17}O-labelled hexanol mixture in 590 µL of $CDCl_3$. 30 degree ^{13}C pulse with power-gated WALTZ-16 ^{1}H composite pulse decoupling, spectral width 260 ppm, 256 scans, 4 dummy scans, 2 s recycle delay, 131072 complex data points, acquisition time 1.68 s, 13C transmitter set to 110 ppm, 1H transmitter set to 4 ppm, 2 x zero-filled with 0.3 Hz line-broadening applied.

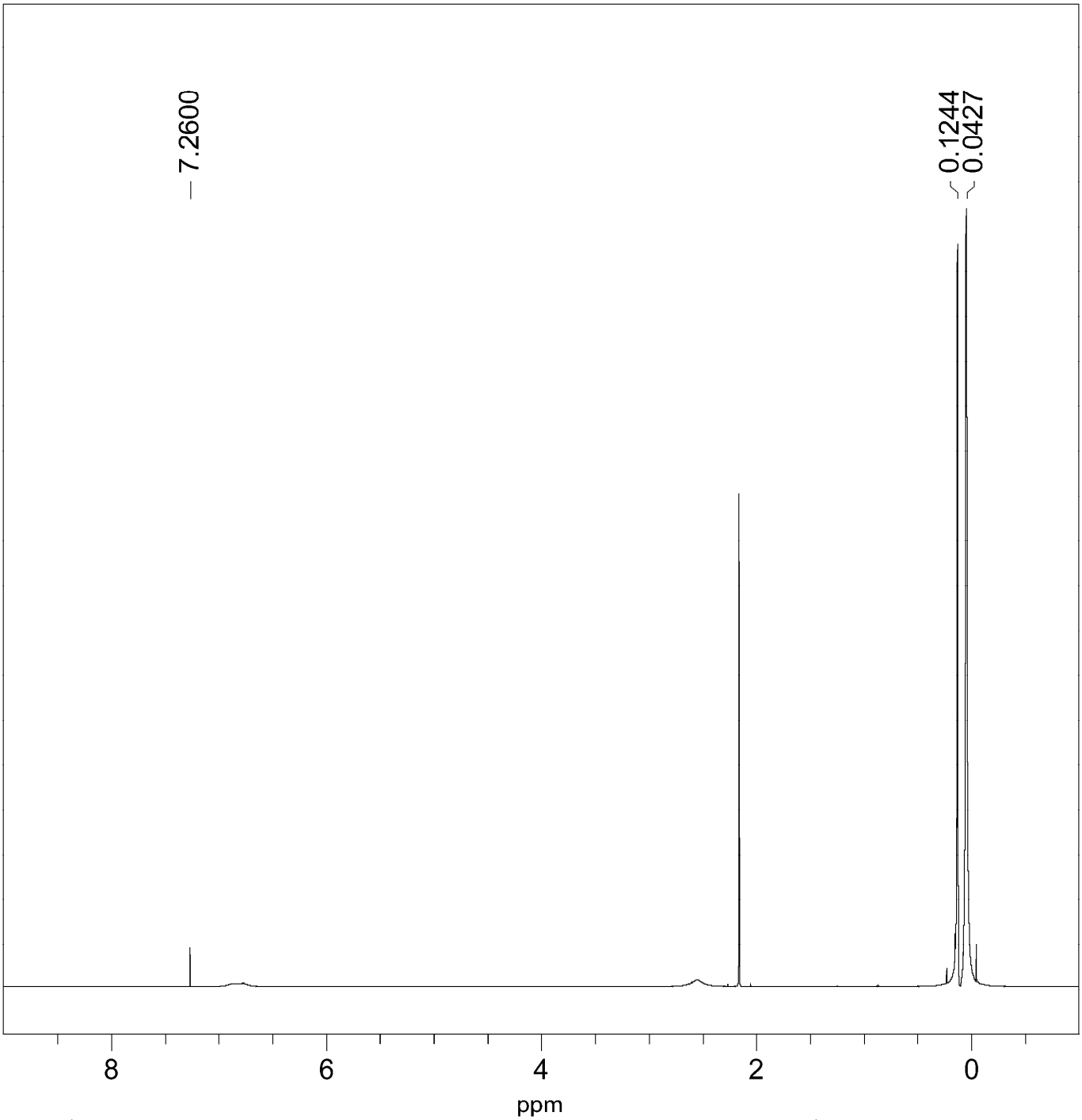

Figure S8. ^{1}H NMR spectrum of hexamethyl siloxane and trimethyl silanol in in $CDCl_3$. 90 degree ^{1}H pulse, spectral width 16 ppm, 16 scans, 1 s recycle delay, 65536 complex data points, acquisition time 3.40 s, ^{1}H transmitter set to 3 ppm, 2 x zero-filled with 0.1 Hz line-broadening applied.

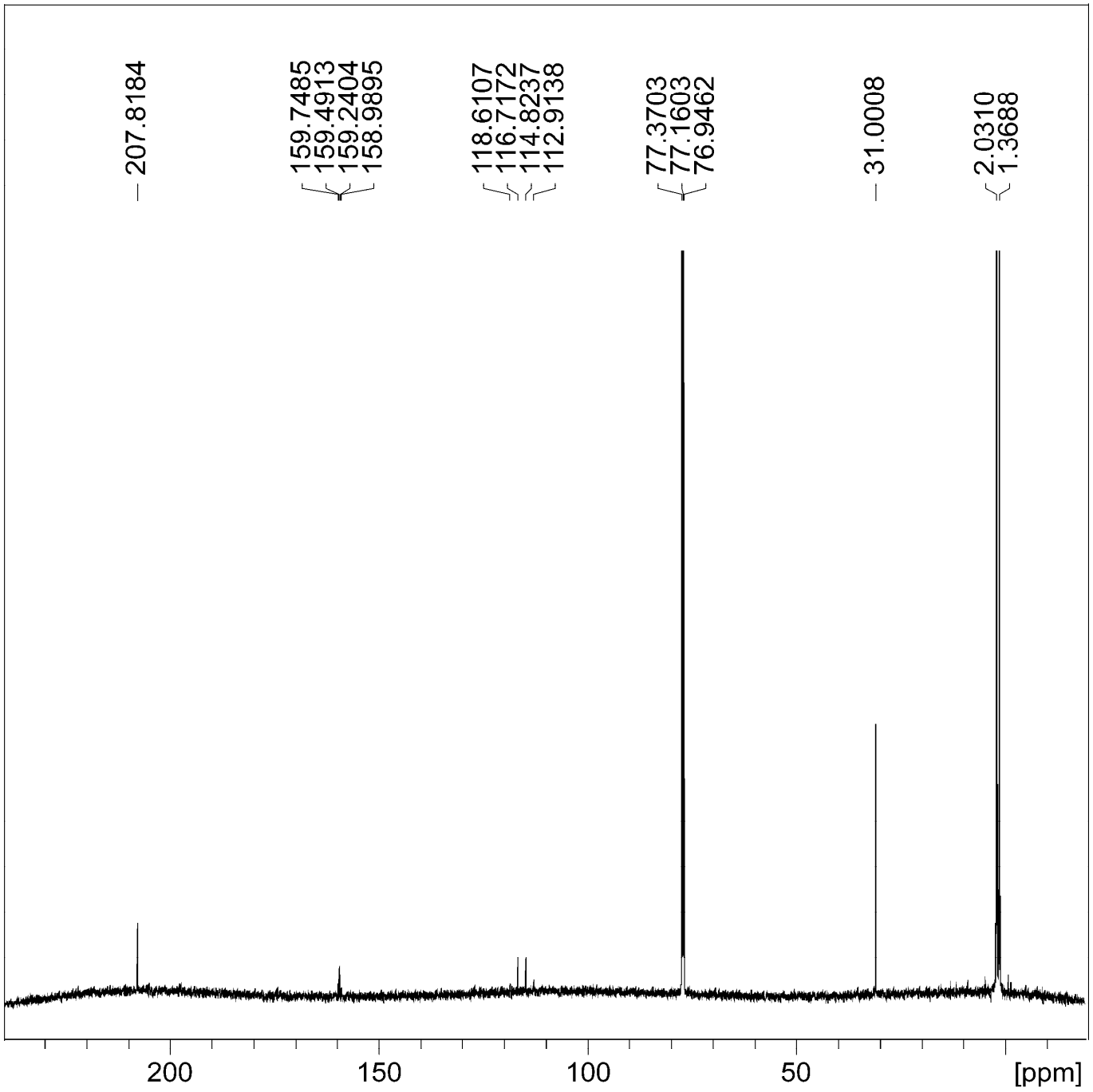

Figure S9. $^{13}C\{^{1}H\}$ NMR spectrum of hexamethyl siloxane and trimethyl silanol in $CDCl_3$. Note acetone impurity (31.0, 207.8 ppm) and trifluoro acetamide (quartets @ 159.3, 115.7 ppm). 30 degree ^{13}C pulse with power-gated WALTZ-16 ^{1}H composite pulse decoupling, spectral width 260 ppm, 64 scans, 4 dummy scans, 2 s recycle delay, 131072 complex data points, acquisition time 1.68 s, ^{13}C transmitter set to 110 ppm, ^{1}H transmitter set to 4 ppm, 2 x zero-filled with 0.3 Hz line-broadening applied.

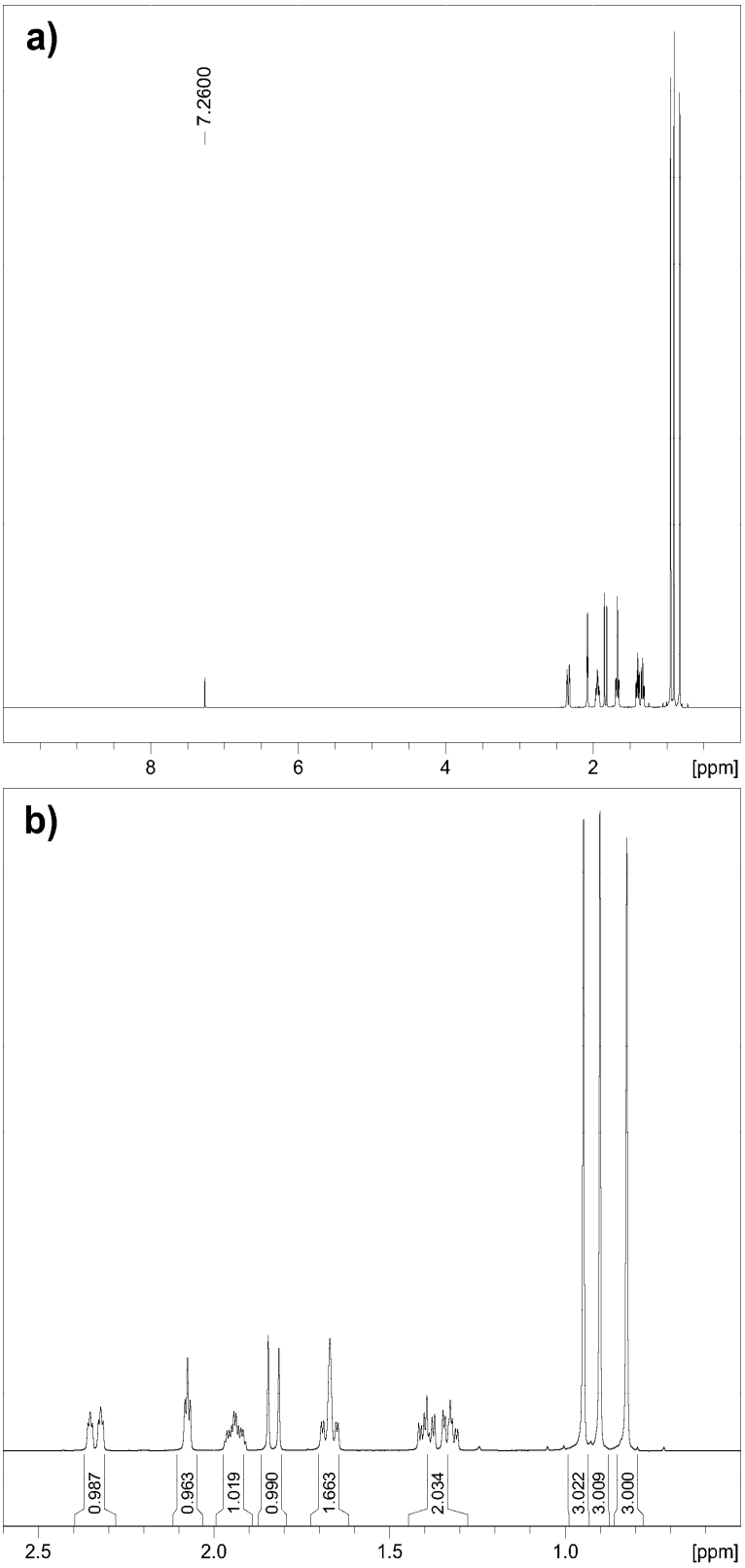

Figure S10. ^{1}H NMR spectrum of 7 mg of unlabelled camphor in 590 µL of $CDCl_3$ and 10 µL of unlabelled water. 90 degree ^{1}H pulse, spectral width 16 ppm, 16 scans, 1 s recycle delay, 65536 complex data points, acquisition time 3.40 s, ^{1}H transmitter set to 3 ppm, 2 x zero-filled with 0.1 Hz line-broadening applied. **a)** 0 - 10 ppm region, **b)** expansion of 0.5 – 2.6 ppm region.

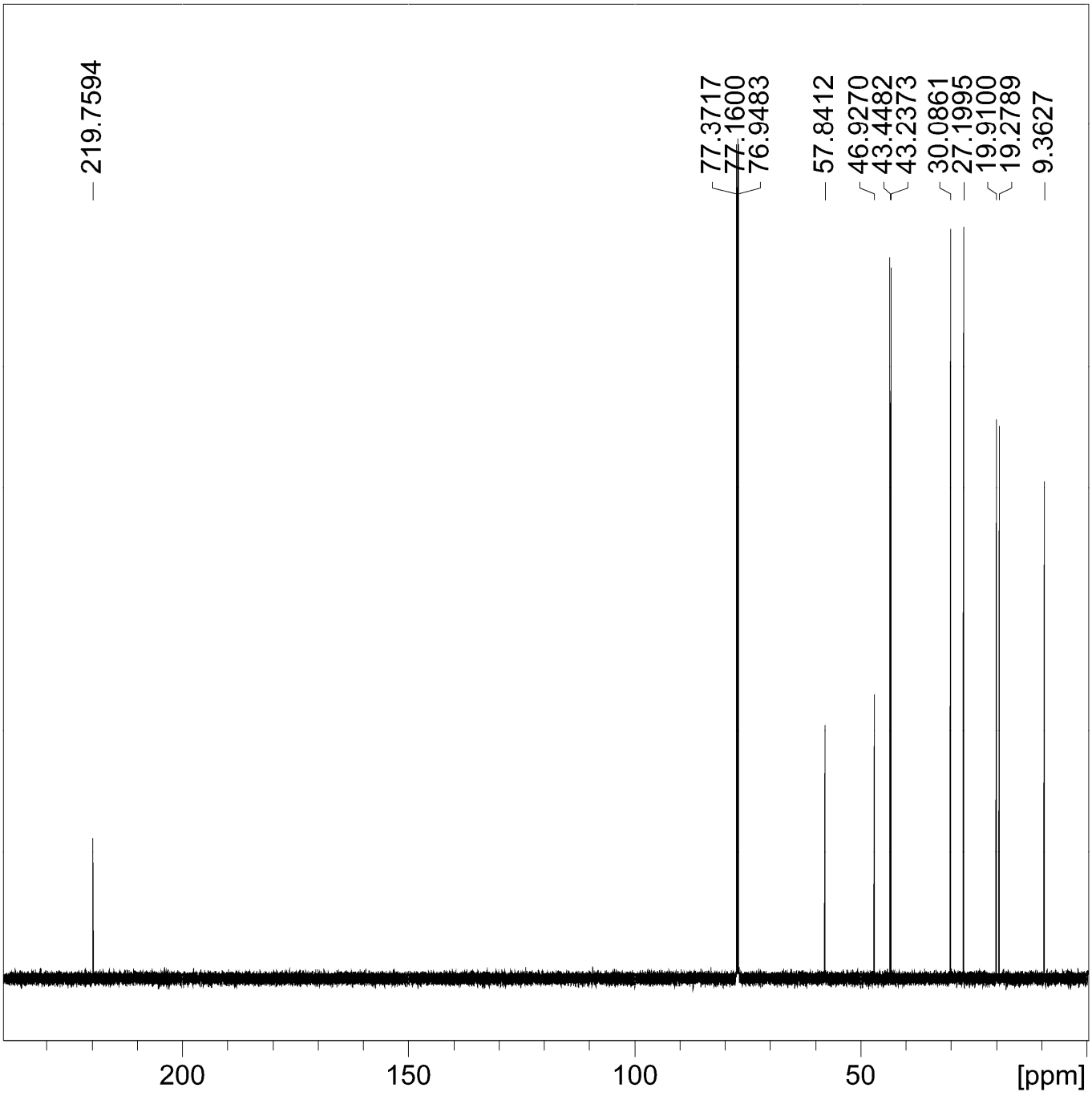

Figure S11. $^{13}C\{^{1}H\}$ NMR spectrum of 7 mg of unlabelled camphor in 590 µL of $CDCl_3$ and 10 µL of unlabelled water. 30 degree ^{13}C pulse with power-gated WALTZ-16 ^{1}H composite pulse decoupling, spectral width 260 ppm, 256 scans, 4 dummy scans, 2 s recycle delay, 131072 complex data points, acquisition time 1.68 s, ^{13}C transmitter set to 110 ppm, ^{1}H transmitter set to 4 ppm, 2 x zero-filled with 0.3 Hz line-broadening applied.

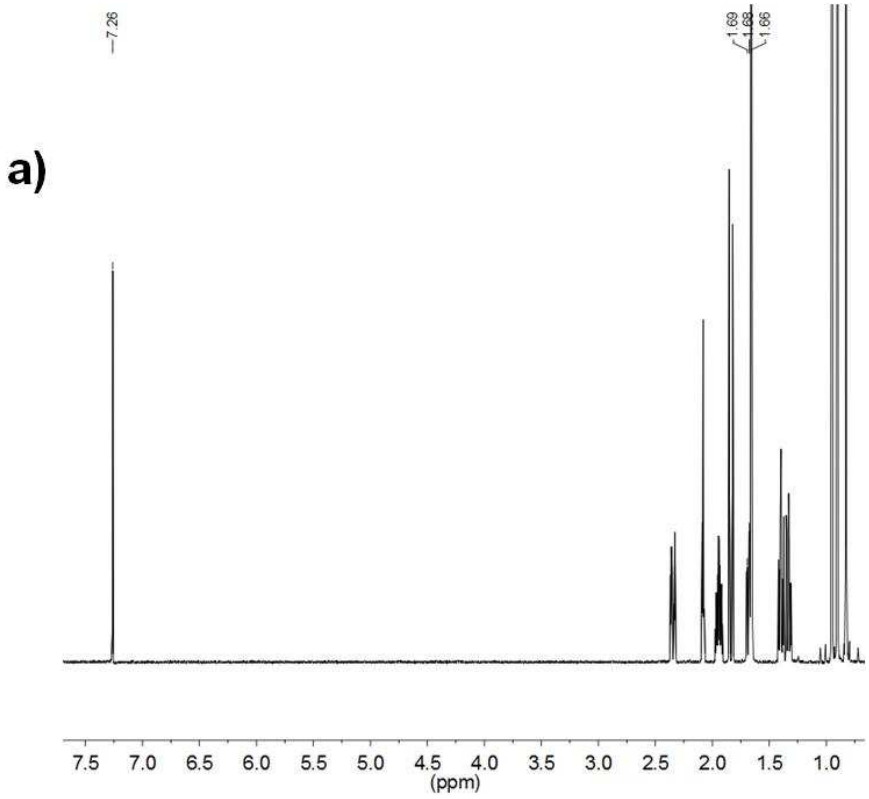
a)
7.26
1.69
1.68
1.66
7.5 7.0 6.5 6.0 5.5 5.0 4.5 4.0 3.5 3.0 2.5 2.0 1.5 1.0
(ppm)

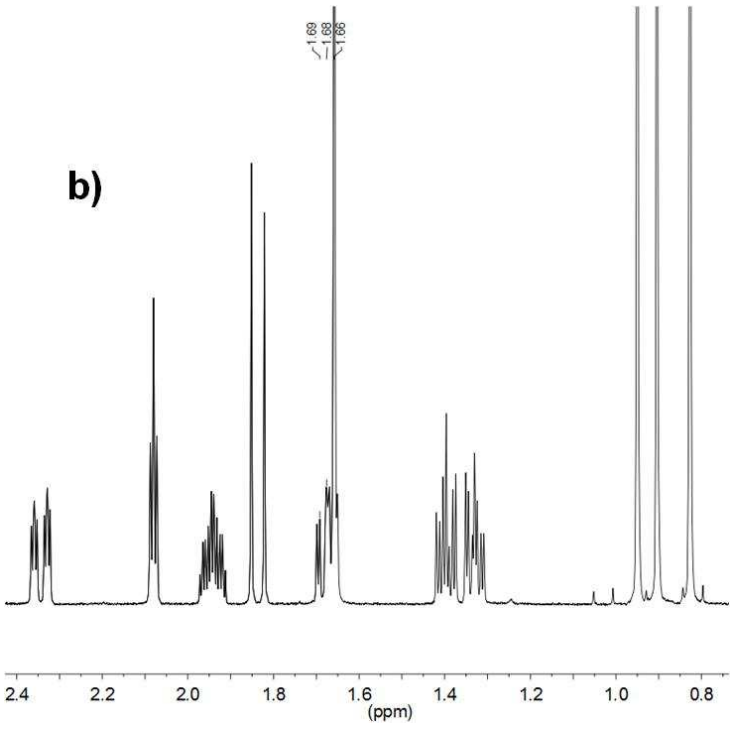
b)
1.69
1.68
1.66
2.4 2.2 2.0 1.8 1.6 1.4 1.2 1.0 0.8
(ppm)

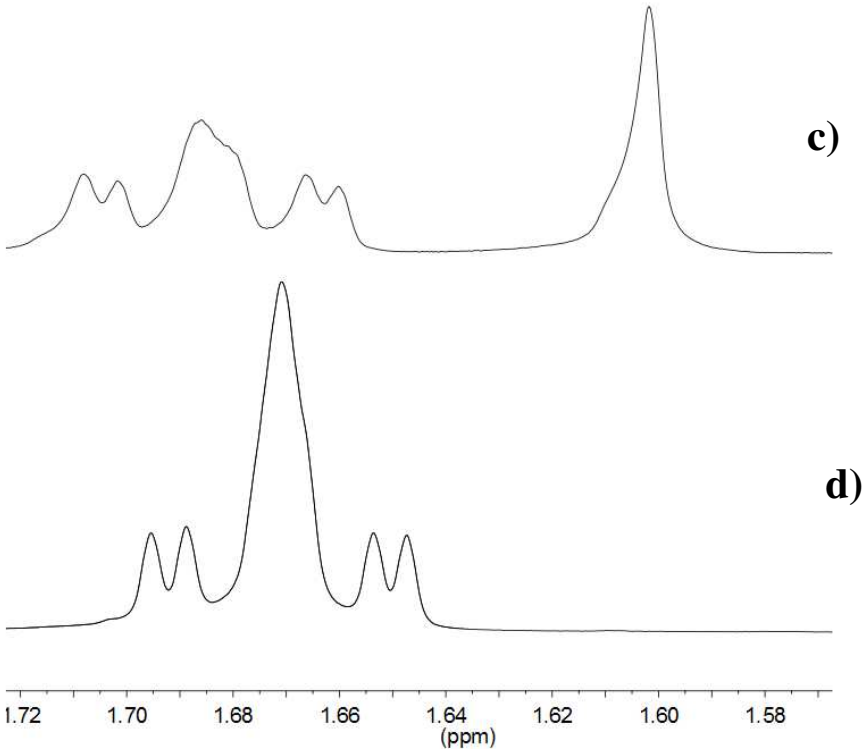

Figure S12. ^{1}H NMR spectrum of 7 mg of ^{17}O-labelled camphor in 590 µL of $CDCl_3$ and 10 µL of ^{17}O-labelled water. 90 degree ^{1}H pulse, spectral width 16 ppm, 16 scans, 1 s recycle delay, 65536 complex data points, acquisition time 3.40 s, ^{1}H transmitter set to 3 ppm, 2 x zero-filled with 0.1 Hz line-broadening applied. **a)** 1 – 7.5 ppm region, **b)** expansion of 0.8 – 2.4 ppm region and **c**) & **d**) Hydration of camphor (expansion of 1.6 – 1.72 ppm region): **c**) camphor before hydration, a singlet at 1.59 ppm was observed **d**) after hydration of camphor, the peak height at 1.67 ppm increased.

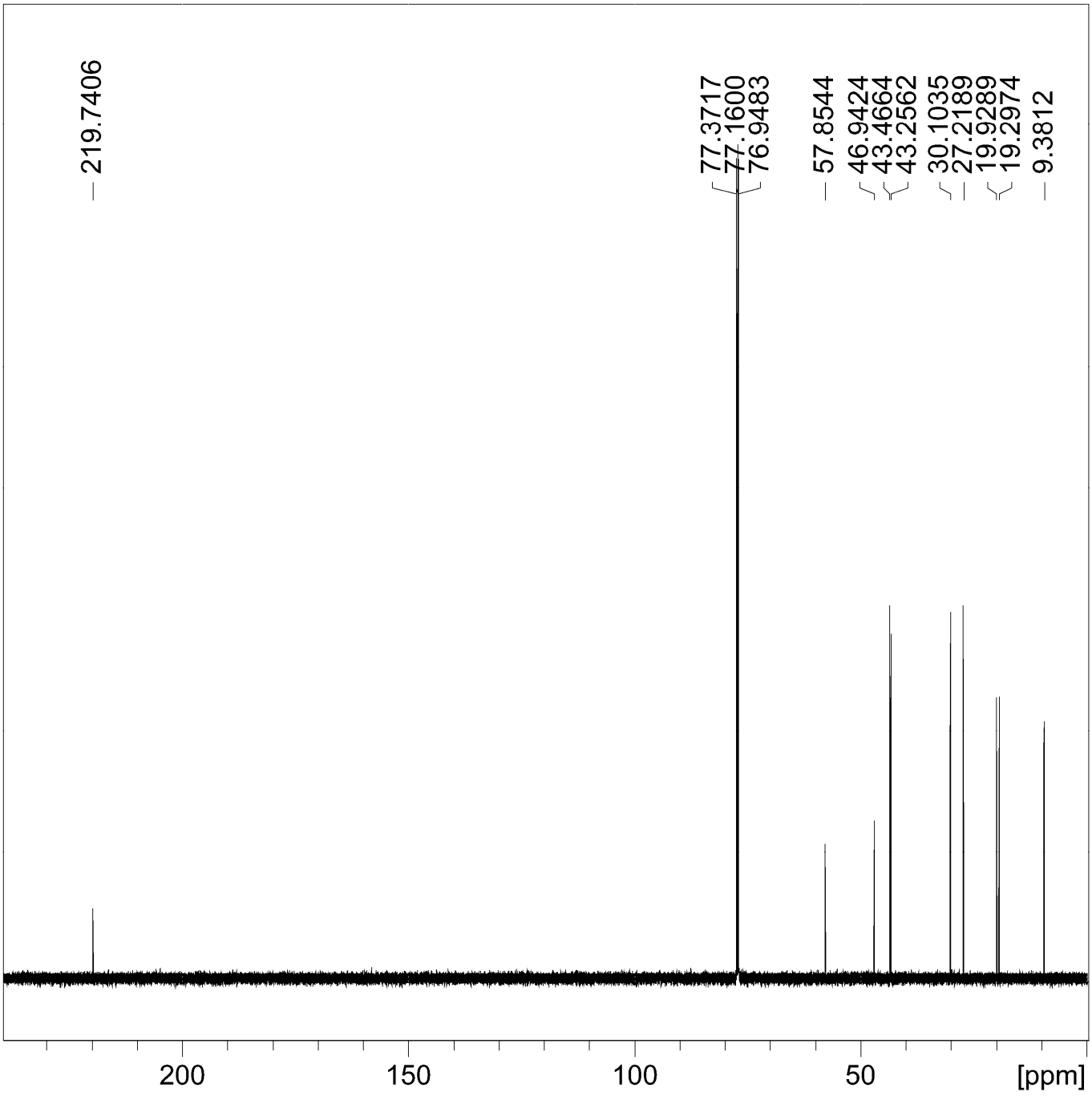

Figure S13. $^{13}C\{^{1}H\}$ NMR spectrum of 7 mg of ^{17}O-labelled camphor in 590 µL of $CDCl_3$ and 10 µL of ^{17}O-labelled water. 30 degree ^{13}C pulse with power-gated WALTZ-16 ^{1}H composite pulse decoupling, spectral width 260 ppm, 256 scans, 4 dummy scans, 2 s recycle delay, 131072 complex data points, acquisition time 1.68 s, 13C transmitter set to 110 ppm, 1H transmitter set to 4 ppm, 2 x zero-filled with 0.3 Hz line-broadening applied.

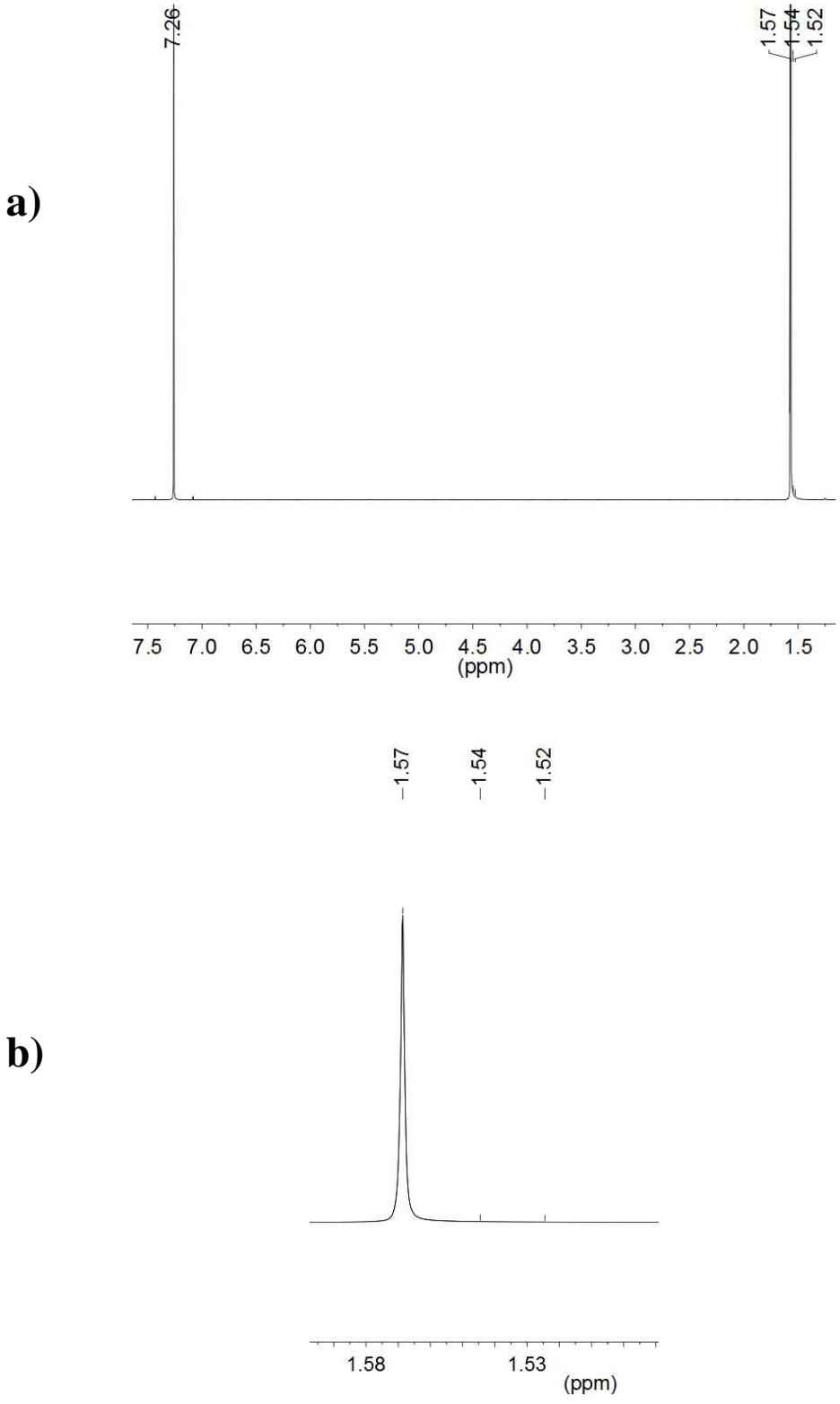

Figure S14. ^{1}H NMR of 3 µL of ^{17}O-labeled water (>90% enriched) dissolved in 540 µL of $CDCl_3$, 90 degree ^{1}H pulse, spectral width 16 ppm, 16 scans, 1 s recycle delay, 65536 complex data points, acquisition time 3.40 s, ^{1}H transmitter set to 3 ppm, 2x zero-filled with 0.1 Hz line-broadening applied : **a**) 1.5-7.5 ppm region, **b**) 1.52-1.60 ppm (expanded)

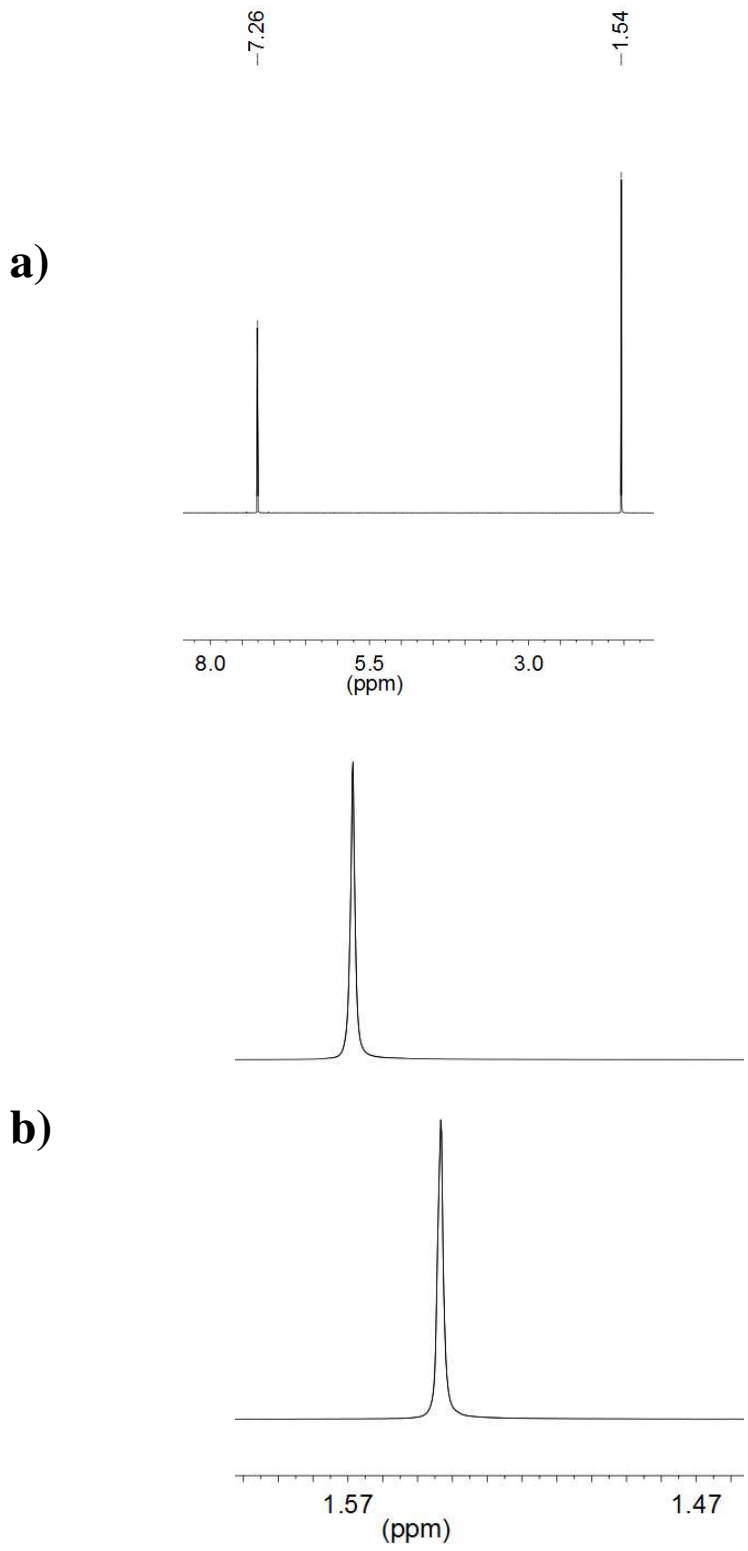

Figure S15. a) ^{1}H NMR of 3 µL of non-labeled water in 540 µL of $CDCl_3$. 90 degree ^{1}H pulse, spectral width 16 ppm, 16 scans, 1s recycle delay, 65536 complex data points, acquisition time 3.40 s, ^{1}H transmitter set to 3 ppm, 2 x zero-filled with 0.1 Hz line-broadening applied b) Stacked ^{1}H NMR spectra of labeled and non-labeled water in $CDCl_3$

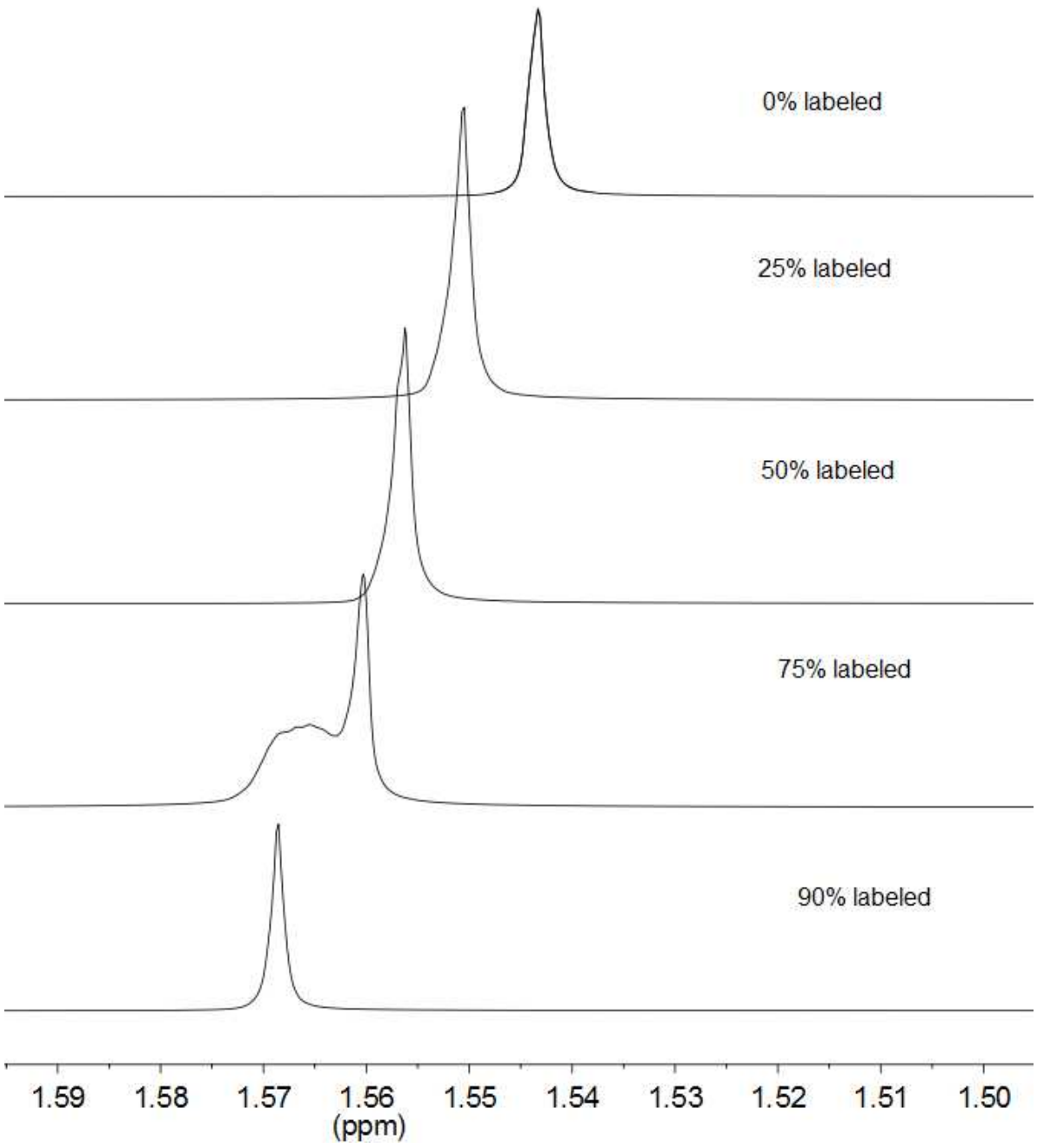

Figure S16. ^{1}H NMR (stacked) spectra of 0-90% labeled water. 90 degree ^{1}H pulse, spectral width 16 ppm, 16 scans, 1 s recycle delay, 65536 complex data points, acquisition time 3.40 s, ^{1}H transmitter set to 3 ppm, 2 x zero-filled with 0.1 Hz line-broadening applied

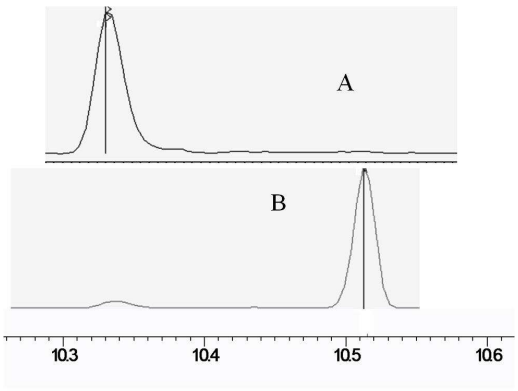

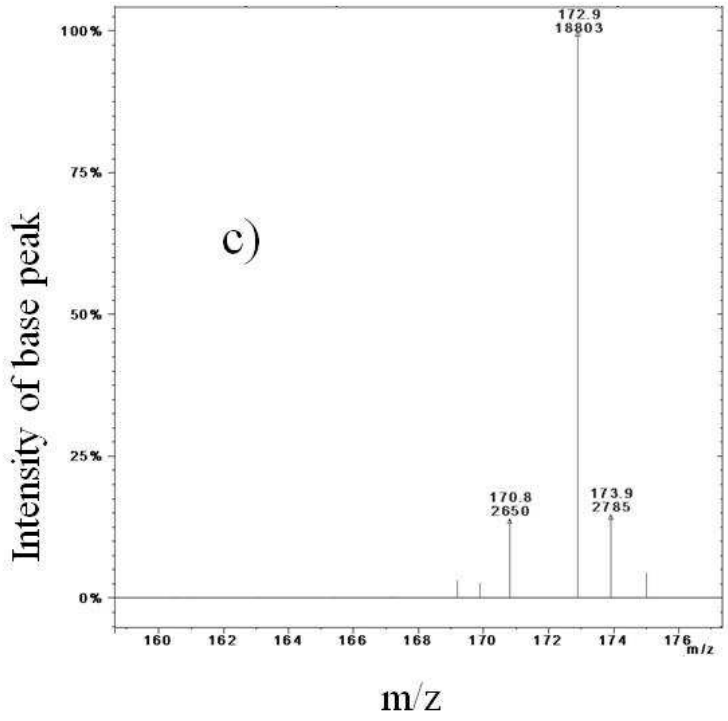

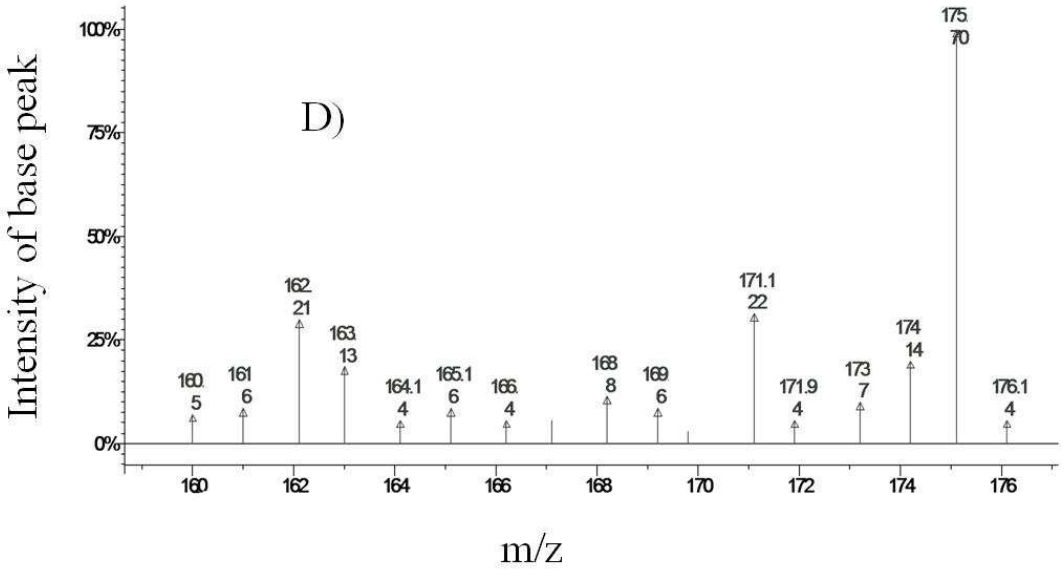

Figure S17. GC-MS analysis of commercial hexanol and ^{17}O labeled hexanol.

A) GC-MS trace (ions displayed) of commercial hexanol B) GC-MS trace (ions displayed) of 1-^{17}O-hexanol
C) Mass spectrum of commercial hexanol (see text for list of ions; m/z =173 = M-1). D) Mass spectrum of 1-^{17}O-hexanol

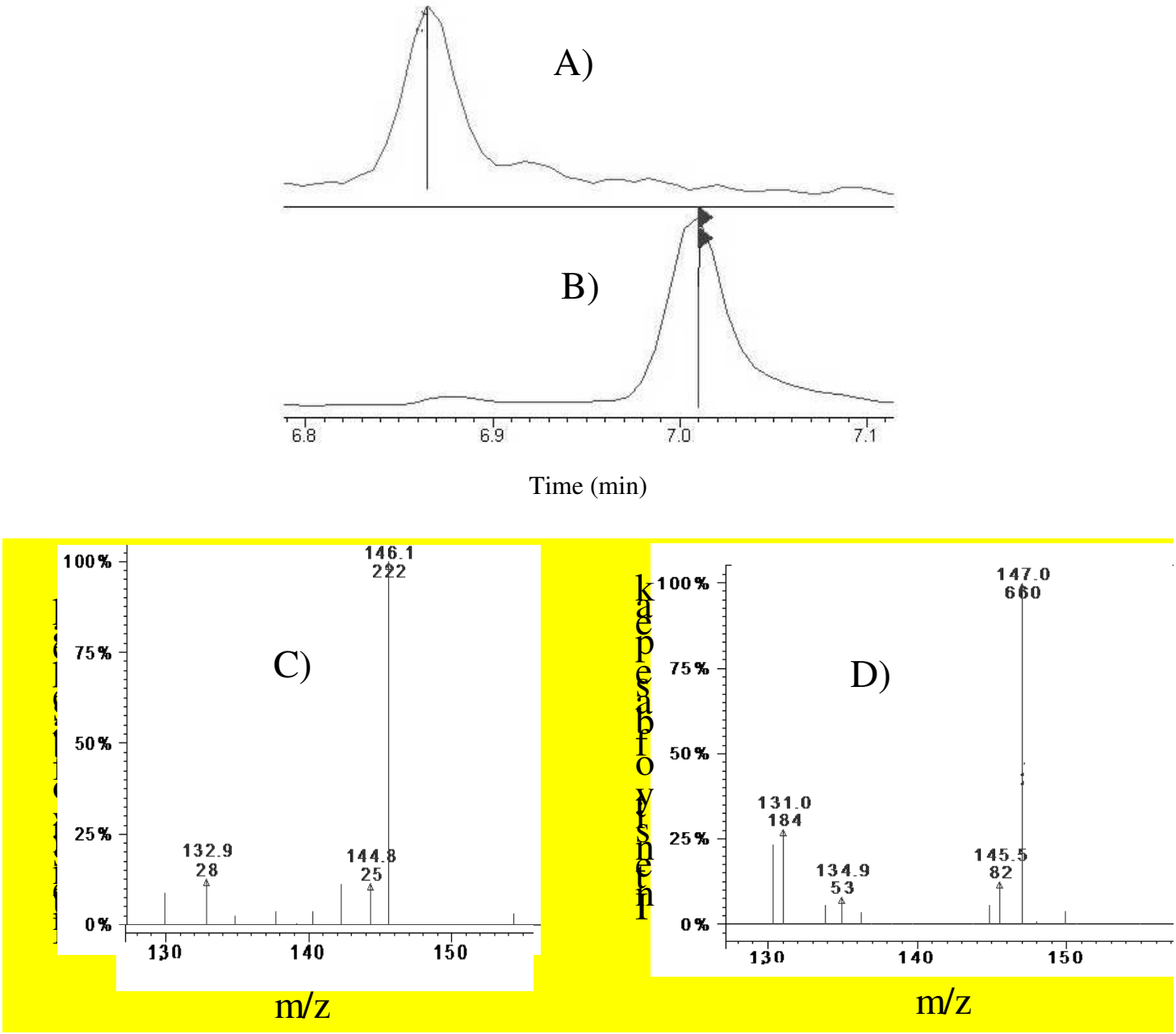

Figure S18. A) GC-MS trace (ions displayed) of unlabelled hexamethyl disiloxane. B) GC-MS trace (ions displayed) of ^{17}O-hexamethyl disiloxane (see text for list of ions, m/z = 147 = M-CH_4). C) Mass spectrum of unlabelled hexamethyl disiloxane. D) Mass spectrum of ^{17}O-hexamethyl disiloxane (see text for list of ions, m/z = 147 = M-CH_4).

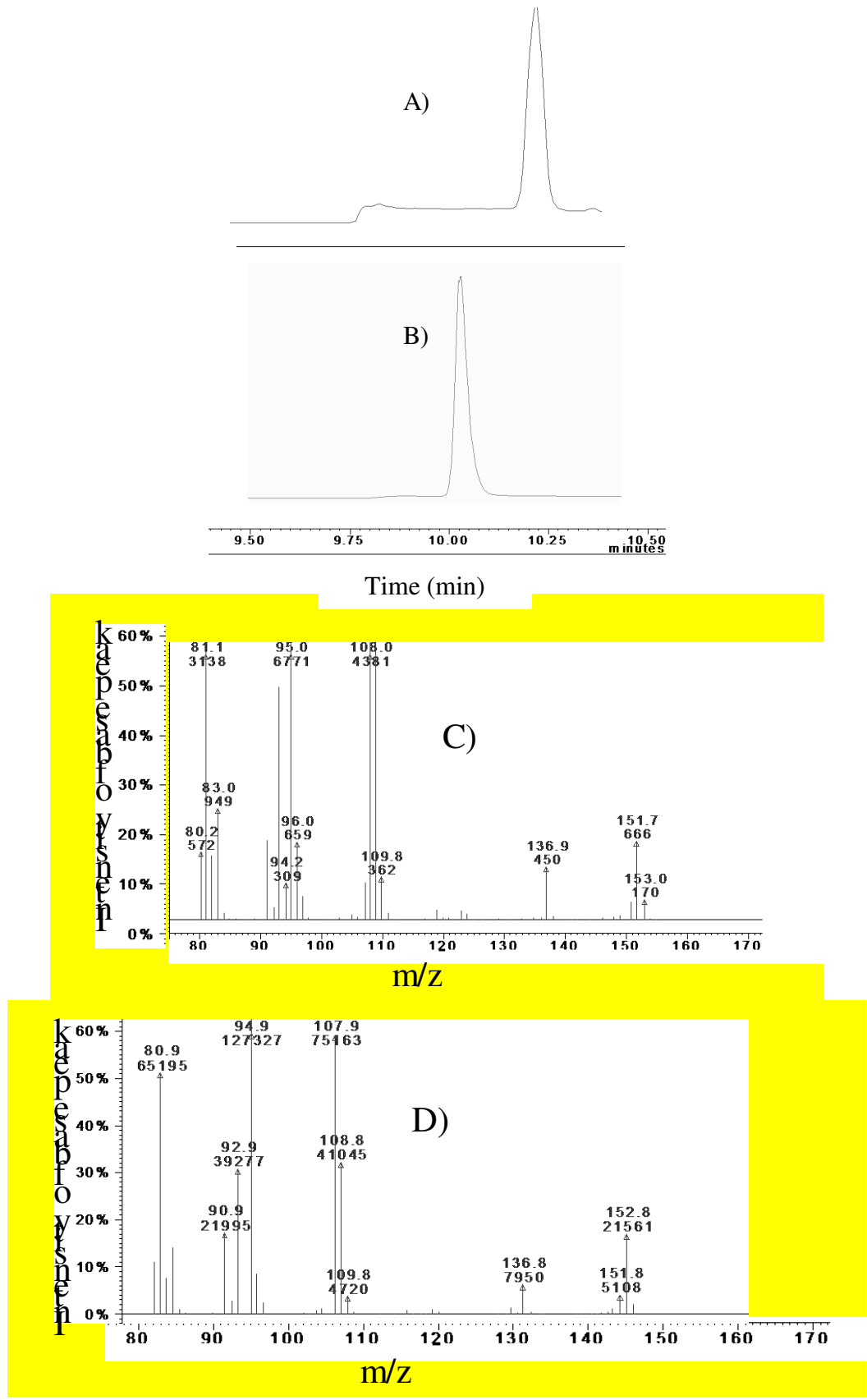

Figure S19. A) GC-MS trace (ions displayed) of unlabelled camphor. B) GC-MS trace (ions displayed) of unlabelled camphor. C) Mass spectrum of unlabelled camphor. D) Mass spectrum of ^{17}O-labelled camphor (see text for list of ions).

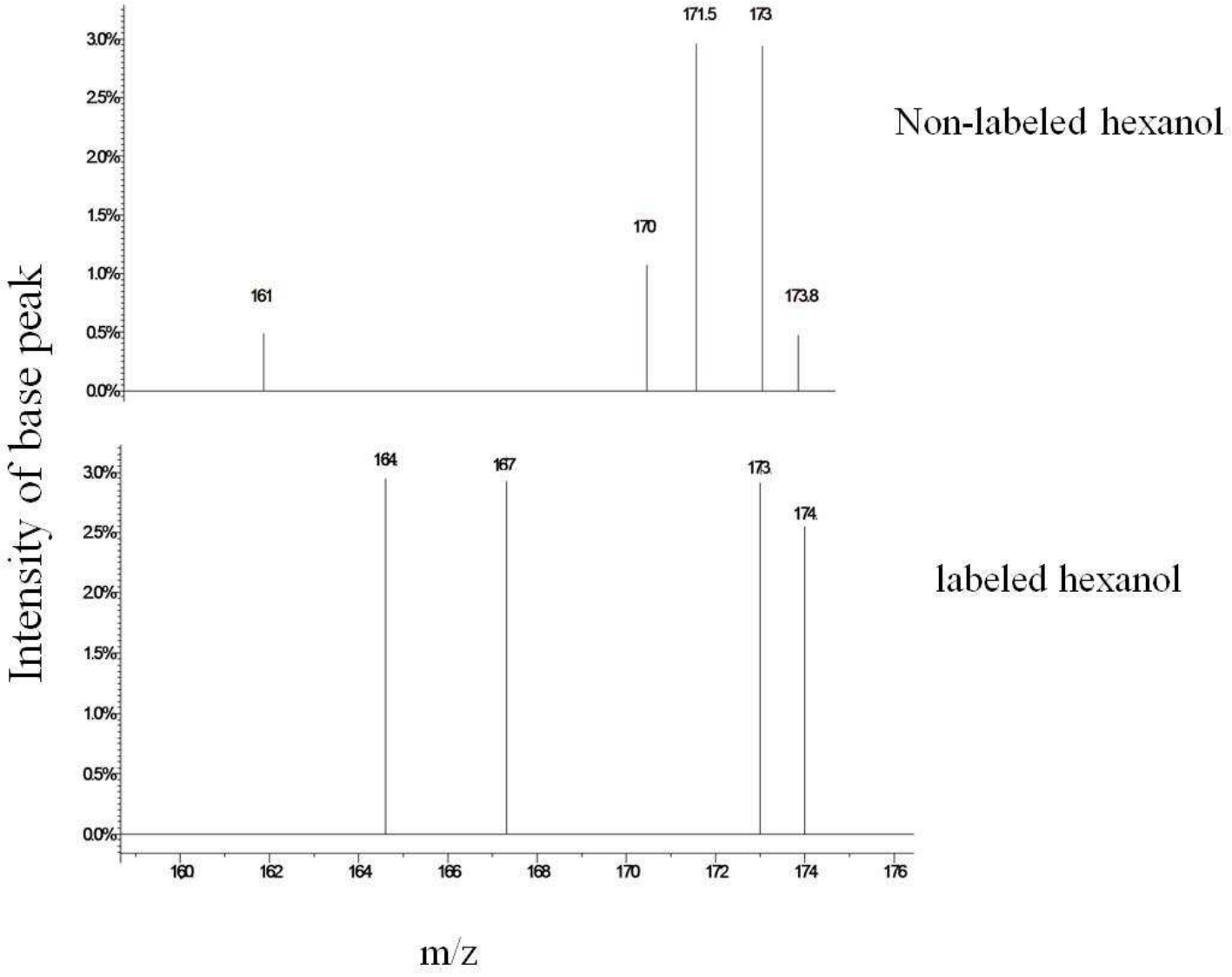

Figure S20. The MS-MS analysis of the parent ion 173 for the labeled and non-labeled hexanols

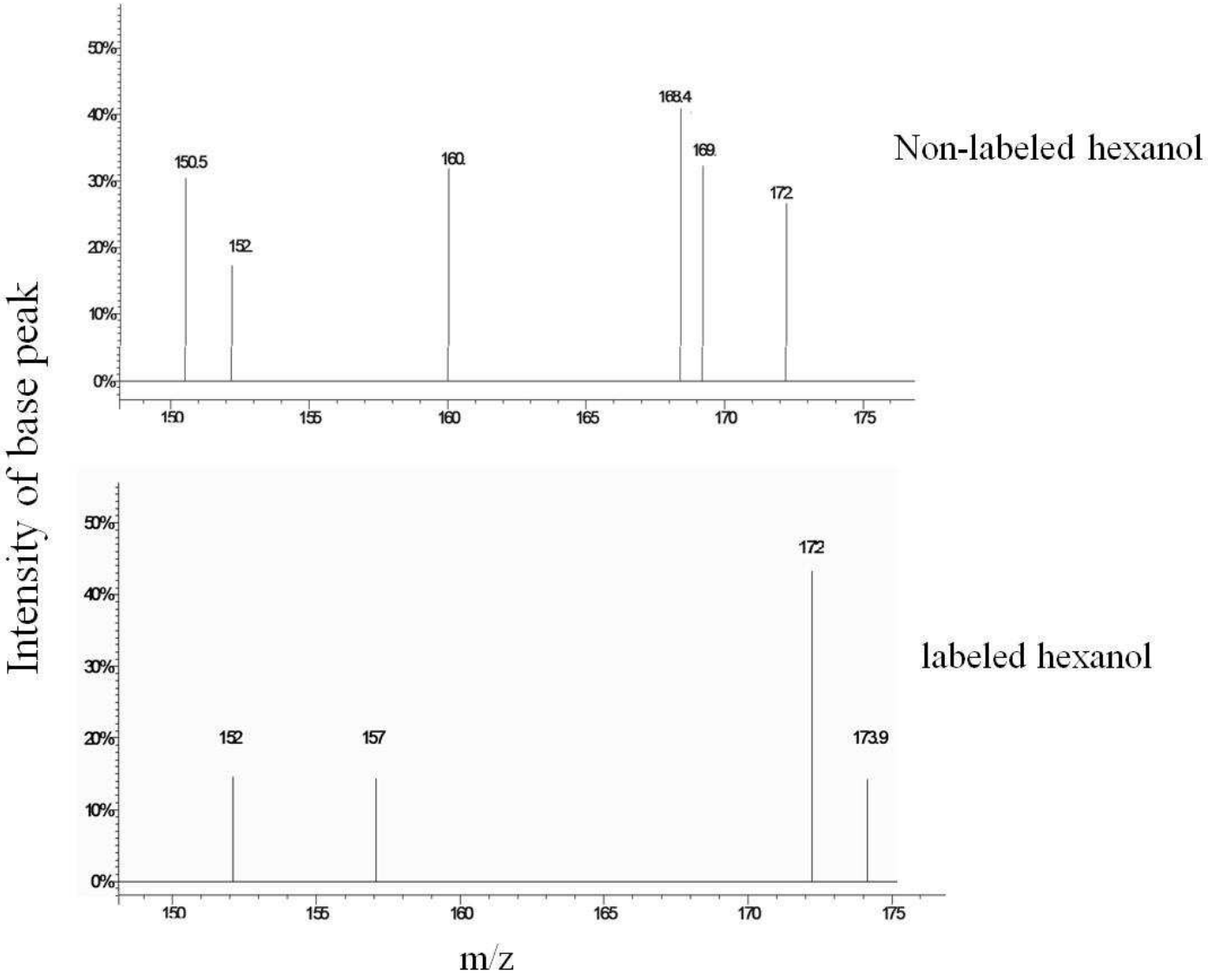

Figure S21: The MS-MS analysis of the parent ion 174 for the labeled and non-labeled hexanols

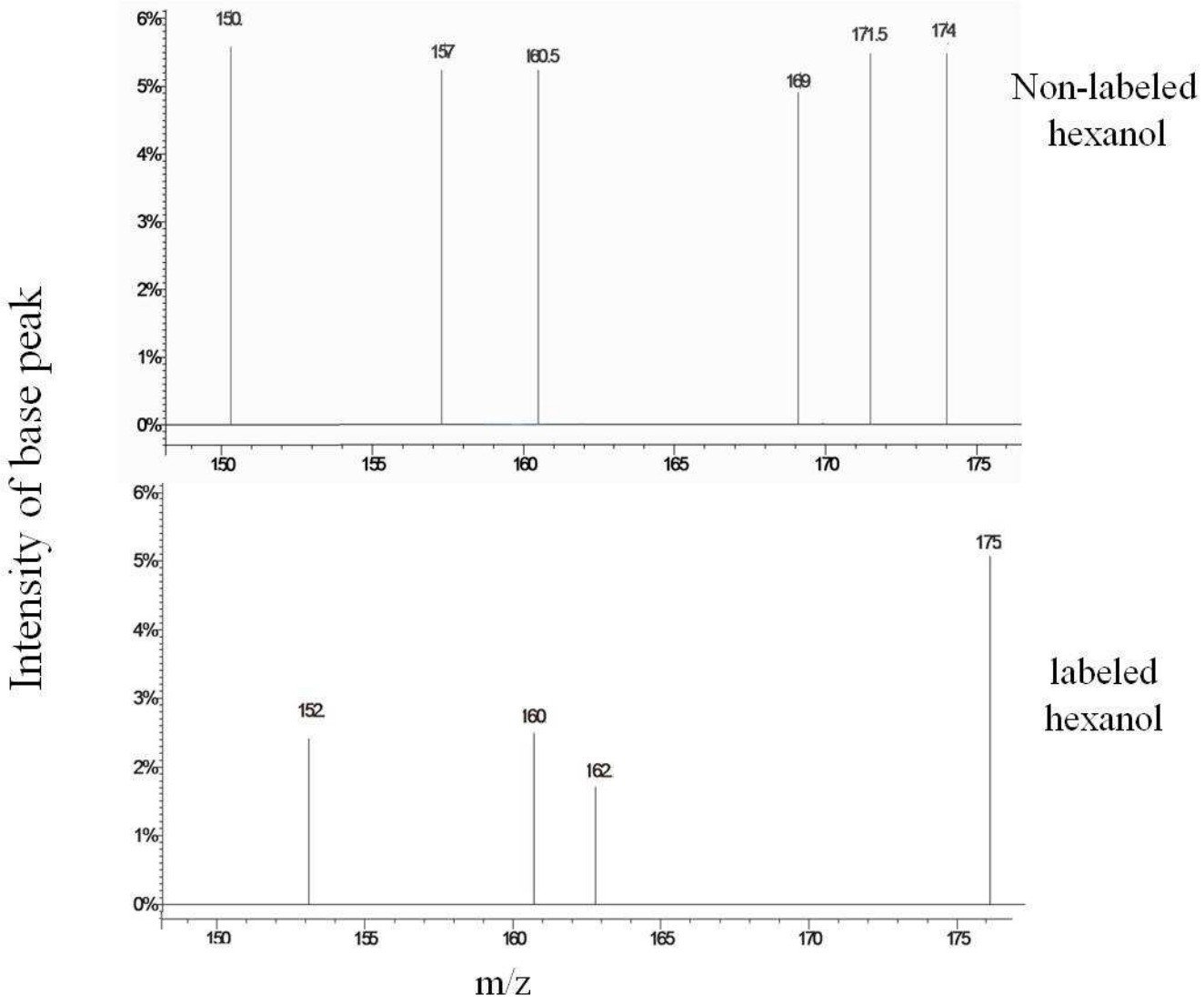

Figure **S22**: The MS-MS analysis of the parent ion 175 for the labeled and non-labeled hexanols

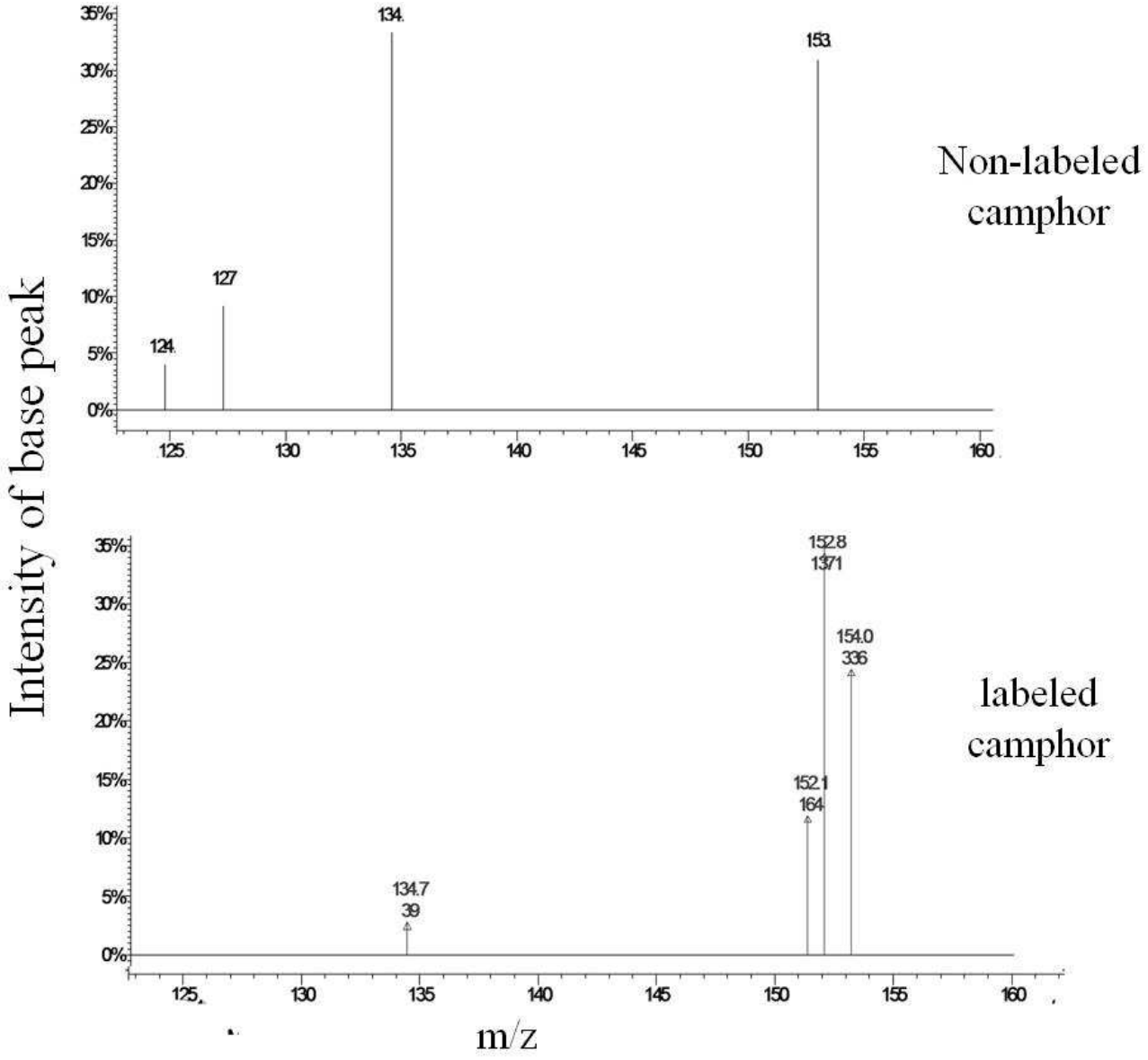

Figure **S23**: The MS-MS analysis of the parent ion 152 for the labeled and non-labeled camphor

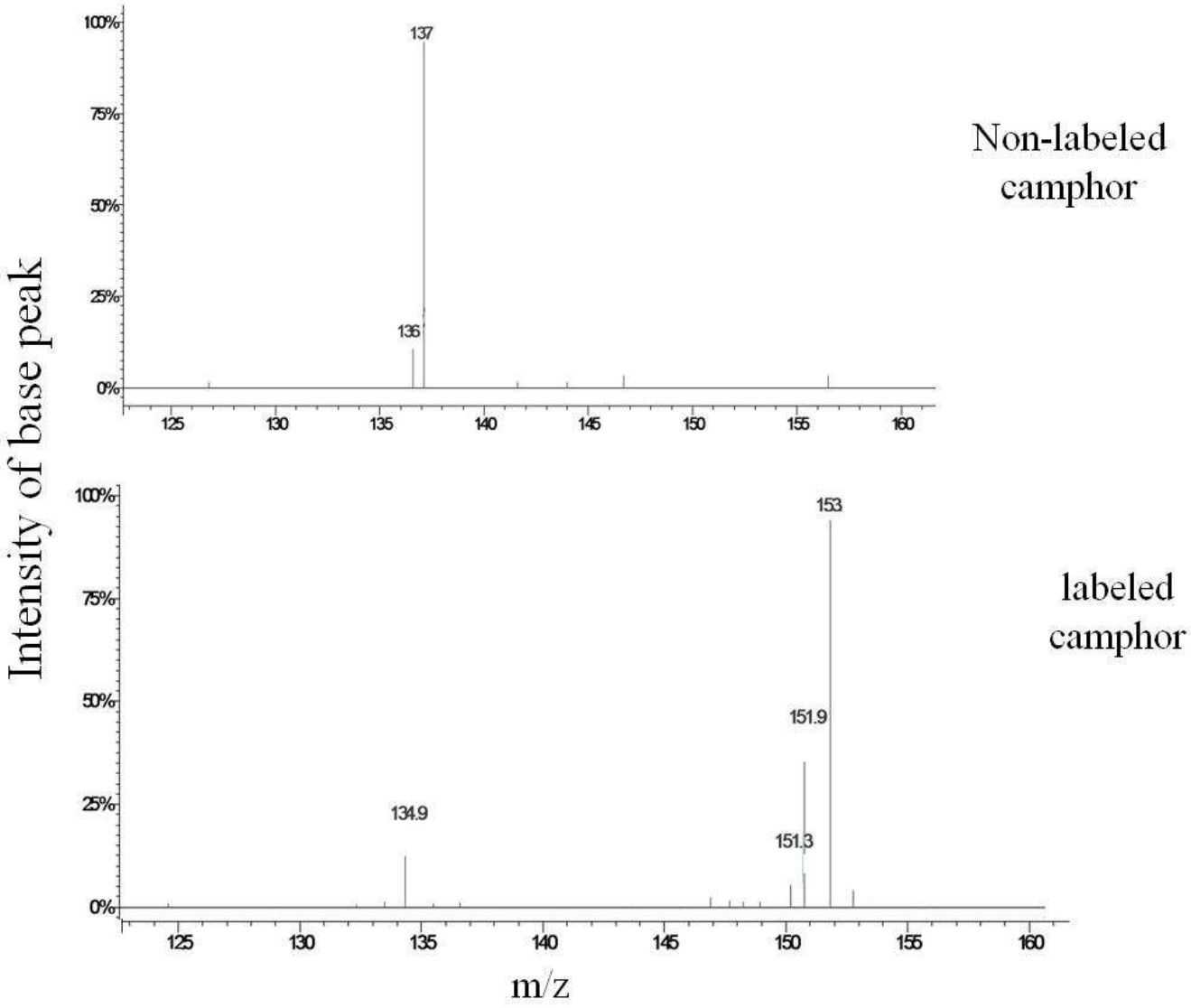

Figure **S24**: The MS-MS analysis of the parent ion 153 for the labeled and non-labeled camphor

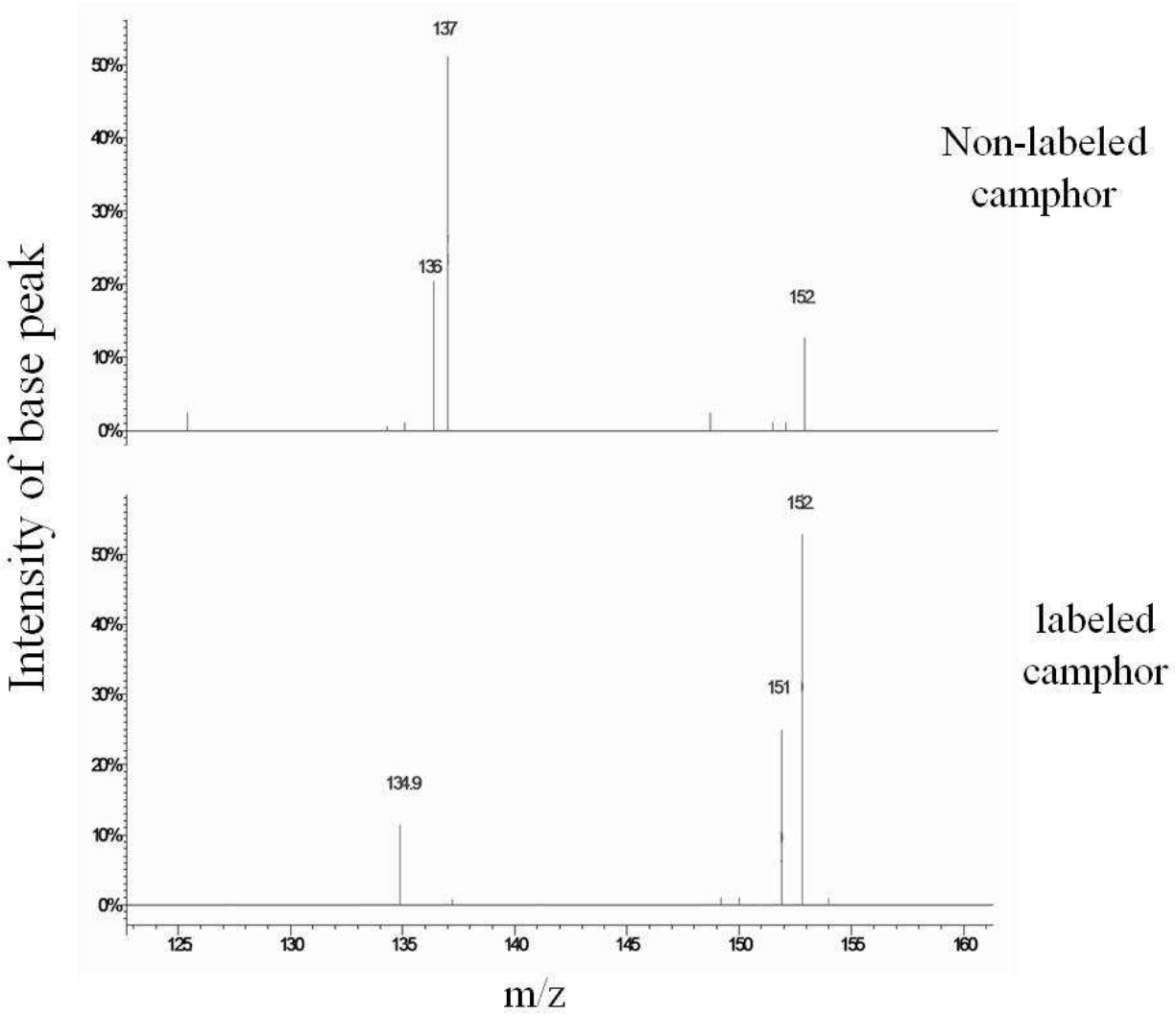

Figure **S25**: The MS-MS analysis of the parent ion 154 for the labeled and non-labeled camphor

References.

(1) Gottlieb, H. E.; Kotlyar, V.; Nudelman, A. *J. Org. Chem.* **1997**, *62*, 7512-7515.
(2) Atkins, W. M.; Sligar, S. G. *Biochemistry* **1988**, *27*, 1610-1616.
(3) Hildebraunt, A. G.; Roots, I. *Arch. Biochem. Biophys.* **1975**, *171*, 385-397.